Nonperturbative evaluation for anomalous dimension in 2-dimensional $O(3)$ sigma model

Sergio Calle Jimenez,[1] Makoto Oka,[1,2] and Kiyoshi Sasaki[1]

[1]*Department of Physics, Tokyo Institute of Technology, Tokyo 152-8551, Japan*
[2]*Advanced Science Research Center, Japan Atomic Energy Agency, Tokai, Ibaraki 319-1195, Japan*

(Received 4 February 2018; published 11 June 2018)

We nonperturbatively calculate the wave-function renormalization in the two-dimensional $O(3)$ sigma model. It is evaluated in a box with a finite spatial extent. We determine the anomalous dimension in the finite-volume scheme through an analysis of the step-scaling function. Results are compared with a perturbative evaluation, and reasonable behavior is observed.

DOI: 10.1103/PhysRevD.97.114506

I. INTRODUCTION

In the late 1980s and early 1990s methods were developed to extract information at infinite volume from the information about a system in a finite box. One way is to calculate the scattering phase shift [1], and another is to determine the running coupling constant [2]. The latter describes a renormalization group (RG) evolution of the renormalized coupling as a response to changes in the box size. The workability of this method might give us foresight into the existence of an RG equation that describes the box-size dependence of the N-point Green function. It will be useful to describe a spatially extended object in a finite box; examples include a deuteron and an Efimov system [3]. For the latter, the infinite size of the object is essential, and thus we cannot avoid a discussion of the box-size dependence in a study with a lattice simulation.

The end goal of our study is to establish such an RG equation. For this purpose, we use the two-dimensional $O(n)$ sigma model. However, until now the wave-function renormalization has not been discussed in the context where the system has been put in a finite box. To establish an RG equation, one might need information about the scale dependence of the wave-function renormalization, which is called the anomalous dimension. The present work aims to give a nonperturbative evaluation of the anomalous dimension as a first step in constructing the RG equation.

Before we begin, we should summarize the basic properties of the two-dimensional $O(n)$ sigma model [4] from the standpoint of perturbative studies. Renormalizability and asymptotic freedom were established in the middle 1970s [5,6]. Asymptotic freedom is important to guarantee the applicability of the perturbative expansion in the high-energy region. Renormalization above two dimensions was also discussed in Refs. [7,8]. The infrared (IR) divergence was regularized with a magnetic field in these studies. A vanishing of the magnetic field activates the IR divergence again. However, renormalization in the minimal subtraction (MS) scheme [9] requires only the cancellation of ultraviolet (UV) divergence. If we restrict ourselves to evaluating the renormalization factor, the IR divergence is not a problem. On the other hand, if we focus on a physical quantity like a mass gap, the IR divergence is a serious problem.

The IR divergence originates from the low dimensionality of the system. The Mermin-Wagner theorem forbids spontaneous symmetry breaking in two dimensions [10]. The perturbative expansion with a fixed direction for the magnetization cannot be justified. As a result, the IR divergence remains in the Green function of the pion mode. It was conjectured by Elitzur [11] and proved by David [12] that the $O(n)$-invariant Green function including the sigma mode is IR finite. Then, the $O(n)$-invariant Green function in a finite box was discussed, and the value of the mass gap was evaluated [2,13–16]. In these studies, particular attention was paid to the treatment of the zero mode. There are several methods, including adding compact extra dimensions [13], separating the collective motion of the magnetization [14], using a background field [15,16], or introducing the IR-cutoff mass by using lattice regularization [2]. We add that some of these works are more recent than others [17–20].

At present, there is no difficulty in evaluating the mass gap of the two-dimensional $O(n)$ sigma model in a finite box regardless of whether it is done perturbatively or nonperturbatively. The mass gap can be used to define the renormalized coupling and discuss the scale dependence of it [2]. On the other hand, having the $O(n)$-invariant two-point Green function, it is also easy to evaluate the amplitude. Then, we can define the wave-function renormalization from the

amplitude, and discuss the scale dependence. This is just the theme addressed in the present study.

This article is organized as follows. In Sec. II, we introduce the two-dimensional $O(n)$ sigma model. Then, we briefly describe a renormalization in the finite-volume (FV) scheme and the procedure to determine the evolution of the parameters of the theory. In Sec. III, we explain details of our Monte Carlo simulations. In Sec. IV, we show the results for the wave-function renormalization in addition to results for the renormalized coupling. We also discuss their scale dependence. In Sec. V, we give our conclusions.

II. MODEL, RENORMALIZATION SCHEME, AND SCALE DEPENDENCE

A. Two-dimensional $O(n)$ sigma model

The two-dimensional $O(n)$ sigma model is formally described by the Euclidean action

$$S[\boldsymbol{\phi}] = \frac{1}{2g^2}\int d^2x \partial_\mu \boldsymbol{\phi}(x)\cdot\partial_\mu\boldsymbol{\phi}(x) \quad (\mu = 0, 1). \tag{1}$$

Here $\boldsymbol{\phi}(x) = (\phi_i(x), i = 1, \ldots, n)$ is the n-component field with the constraint

$$\boldsymbol{\phi}(x)\cdot\boldsymbol{\phi}(x) = 1. \tag{2}$$

The dot symbol denotes the scalar product of n-component vectors. The system is put in a finite box with temporal extent T and spatial extent L. We assume that T is sufficiently large compared to L. In the present work, we impose the Neumann boundary condition (NBC) for the temporal direction, and the periodic boundary condition (PBC) for the spatial direction,

$$\begin{aligned} &\frac{\partial}{\partial x_0}\boldsymbol{\phi}(x_0, x_1) = 0 \quad (x_0 \in \partial\Lambda_\tau), \\ &\boldsymbol{\phi}(x_0, x_1 + Ln) = \boldsymbol{\phi}(x_0, x_1) \quad (n \in \mathbb{Z}), \end{aligned} \tag{3}$$

where $\partial\Lambda_\tau$ represents the temporal boundary. The reason why we use the NBC in the temporal direction is to realize the $O(n)$-invariant state at $\partial\Lambda_\tau$. As a result, states other than the spin-1 state do not contribute to the two-point Green function. The NBC is also called the free boundary condition.

As we said in Sec. I, the $O(n)$-invariant Green function should be used to avoid the IR divergence. The $O(n)$-invariant two-point Green function is defined by

$$G_{\mathrm{inv}}(x; y) = \langle \boldsymbol{\phi}(x)\cdot\boldsymbol{\phi}(y)\rangle, \tag{4}$$

where the angled brackets refer to the expectation values over the configurations of the $\boldsymbol{\phi}$ field. We consider the zero-momentum projected Green function,

$$G_{\mathrm{inv}}(x_0; y_0) = \frac{1}{L^2}\int dx_1 dy_1 \mathrm{e}^{-ip_1(y_1 - x_1)} G_{\mathrm{inv}}(x; y)\Big|_{p_1=0}. \tag{5}$$

With the NBC for the temporal direction, it can be written as

$$G_{\mathrm{inv}}(x_0; y_0) = A\mathrm{e}^{-M|y_0 - x_0|} + \mathcal{O}(\mathrm{e}^{-(4\pi/L)|y_0 - x_0|}). \tag{6}$$

For our purpose, the mass gap M and the amplitude A are needed. Energies of the excited states are known to be at least $4\pi/L$. With a finite L, they are large enough to ignore the contributions to $G_{\mathrm{inv}}(x_0; y_0)$.

B. Renormalization scheme

The renormalization of the two-dimensional $O(n)$ sigma model is done by the replacement

$$g^2 = Z_{\mathrm{R}}^g g_{\mathrm{R}}^2, \tag{7}$$

$$\boldsymbol{\phi}(z) = (Z_{\mathrm{R}}^\phi)^{1/2}\boldsymbol{\phi}_{\mathrm{R}}(z). \tag{8}$$

Here g_{R}^2 is the renormalized coupling, and $\boldsymbol{\phi}_{\mathrm{R}}(z)$ is the renormalized field. There is a finite arbitrariness in choosing them. This arbitrariness can be removed by setting values for g_{R}^2 and the wave-function renormalization Z_{R}^ϕ at an energy scale μ. Such conditions are called renormalization conditions. The definition of μ in the MS scheme is given in the Appendix.

In the present study, we consider the renormalization conditions at $\mu = 1/L$ as

$$\frac{n-1}{2L} g_{\mathrm{FV}}^2(\mu)\big|_{\mu=1/L} = M, \tag{9}$$

$$Z_{\mathrm{FV}}^\phi(\mu)\big|_{\mu=1/L} = A. \tag{10}$$

M and A are the mass gap and amplitude, respectively, which are determined from the measured value of the $O(n)$-invariant two-point Green function. The renormalized coupling in Eq. (9) was first proposed in Ref. [2] where it was called the FV coupling. In the following, we refer to Eqs. (9) and (10) as the renormalization in the FV scheme. As long as there is no confusion, we write the argument of g_{FV}^2 and Z_{FV}^ϕ as L, but not $1/L$.

The β function and the anomalous dimension describe the μ dependence of the renormalized parameters on the fixed bare parameters g^2 and $\boldsymbol{\phi}(x)$. They are defined as

$$\beta_{\mathrm{R}}(g_{\mathrm{R}}^2) \equiv \mu\frac{d}{d\mu} g_{\mathrm{R}}^2(\mu), \tag{11}$$

$$\gamma_{\mathrm{R}}(g_{\mathrm{R}}^2) \equiv \mu\frac{d}{d\mu}\ln Z_{\mathrm{R}}^\phi(\mu), \tag{12}$$

respectively. In the FV scheme, they are written as

$$\beta_{\rm FV}(g^2_{\rm FV}) = -L\frac{d}{dL}g^2_{\rm FV}(L), \tag{13}$$

$$\gamma_{\rm FV}(g^2_{\rm FV}) = -L\frac{d}{dL}\ln Z^{\phi}_{\rm FV}(L), \tag{14}$$

by using $\mu = 1/L$ in Eqs. (11) and (12).

C. Scale dependence

The step-scaling function (SSF) describes how parameters of a theory evolve when the scale is changed. We consider two types of SSFs: σ^g and σ^ϕ. They are defined through

$$g^2_{\rm FV}(sL) = \sigma^g(s, g^2_{\rm FV}(L)), \tag{15}$$

$$Z^{\phi}_{\rm FV}(sL) = \sigma^{\phi}(s, g^2_{\rm FV}(L))Z^{\phi}_{\rm FV}(L), \tag{16}$$

with a scaling factor s. $\sigma^g(s, g^2_{\rm FV})$ was proposed in Ref. [2], and $\sigma^\phi(s, g^2_{\rm FV})$ is motivated by Ref. [21]. They are related to $\beta_{\rm FV}(g^2_{\rm FV})$ and $\gamma_{\rm FV}(g^2_{\rm FV})$ by

$$\beta_{\rm FV}(\sigma^g(s, g^2_{\rm FV})) = -s\frac{\partial\sigma^g(s, g^2_{\rm FV})}{\partial s}, \tag{17}$$

$$\gamma_{\rm FV}(\sigma^g(s, g^2_{\rm FV})) = -s\frac{\partial\ln\sigma^{\phi}(s, g^2_{\rm FV})}{\partial s}, \tag{18}$$

respectively. However, the SSFs are directly related to values measured in a Monte Carlo simulation, in contrast to $\beta_{\rm FV}(g^2_{\rm FV})$ and $\gamma_{\rm FV}(g^2_{\rm FV})$.

If $\beta_{\rm FV}(g^2_{\rm FV})$ and $\gamma_{\rm FV}(g^2_{\rm FV})$ are perturbatively known, $\sigma^g(s, g^2_{\rm FV})$ and $\sigma^\phi(s, g^2_{\rm FV})$ can be evaluated. Using the abbreviation $u \equiv g^2_{\rm FV}$ to simplify the expression, we consider the perturbative expansions of $\beta_{\rm FV}(u)$ and $\gamma_{\rm FV}(u)$,

$$\beta_{\rm FV}(u) = -u^2\sum_{i=0}^{\infty}\beta_{{\rm FV},i}u^i,$$
$$\gamma_{\rm FV}(u) = -u\sum_{i=0}^{\infty}\gamma_{{\rm FV},i}u^i, \tag{19}$$

and those of the SSFs,

$$\sigma^g(s,u) = u + u\sum_{i=0}^{\infty}\sigma^g_i(s)u^{i+1},$$
$$\sigma^{\phi}(s,u) = 1 + \sum_{i=0}^{\infty}\sigma^{\phi}_i(s)u^{i+1}. \tag{20}$$

By substituting Eqs. (19) and (20) into Eqs. (17) and (18), and by comparing the coefficients at the same order of u, we obtain

$$\sigma^g_0(s) = \beta_{{\rm FV},0}\ln s,$$
$$\sigma^g_1(s) = \beta_{{\rm FV},1}\ln s + \beta^2_{{\rm FV},0}(\ln s)^2,$$
$$\sigma^g_2(s) = \beta_{{\rm FV},2}\ln s + \frac{5}{2}\beta_{{\rm FV},0}\beta_{{\rm FV},1}(\ln s)^2 + \beta^3_{{\rm FV},0}(\ln s)^3, \tag{21}$$

and

$$\sigma^{\phi}_0(s) = \gamma_{{\rm FV},0}\ln s,$$
$$\sigma^{\phi}_1(s) = \gamma_{{\rm FV},1}\ln s + \frac{1}{2}(\beta_{{\rm FV},0} + \gamma_{{\rm FV},0})\gamma_{{\rm FV},0}(\ln s)^2,$$
$$\sigma^{\phi}_2(s) = \gamma_{{\rm FV},2}\ln s + (\beta_{{\rm FV},0}\gamma_{{\rm FV},1} + \gamma_{{\rm FV},0}\gamma_{{\rm FV},1} + \beta_{{\rm FV},1}\gamma_{{\rm FV},0}/2)(\ln s)^2 + \frac{1}{3}(\beta_{{\rm FV},0} + \gamma_{{\rm FV},0})(\beta_{{\rm FV},0} + \gamma_{{\rm FV},0}/2)\gamma_{{\rm FV},0}(\ln s)^3, \tag{22}$$

up to the three-loop order. Note that all of the coefficients in $\sigma^g_i(s)$ and $\sigma^{\phi}_i(s)$ are not independent due to the constraint $\sigma^{g,\phi}(s_2s_1, u) = \sigma^{g,\phi}(s_2, \sigma^g(s_1, u))$.

Later, we will need the perturbative evaluation of $\sigma^{g,\phi}(s,u)$. Using Eq. (20) [with Eqs. (21) and (22)] they are evaluated as

$$\beta_{{\rm FV},0} = \frac{n-2}{2\pi}, \qquad \beta_{{\rm FV},1} = \frac{n-2}{4\pi^2},$$
$$\beta_{{\rm FV},2} = \frac{(n-1)(n-2)}{8\pi^3}, \qquad \gamma_{{\rm FV},0} = -\frac{n-1}{2\pi},$$
$$\gamma_{{\rm FV},1} = 0, \qquad \gamma_{{\rm FV},2} = 0, \tag{23}$$

and $\sigma^{g,\phi}_i(s) = 0$ for $i \geq 3$. We denote these SSFs as $\sigma^{g,\phi}_{\rm P}(s)$. The derivation of Eq. (23) is given in the Appendix.

III. DETAILS OF MONTE CARLO SIMULATIONS

A. Setup

We set $n = 3$. The calculation is performed on the $(T/a)\times(L/a)$ lattice with $T = 5L$. Here a is the lattice spacing, and is determined from the bare coupling g^2. Due to the discretization, the action is changed to

$$S_{\rm lat}[\boldsymbol{\phi}] = -\frac{1}{g^2}\sum_{x,\mu}\boldsymbol{\phi}(x)\cdot\boldsymbol{\phi}(x+\hat{\mu}), \tag{24}$$

where x moves all of the lattice space-time points, and $\hat{\mu}$ is a unit vector in the μ direction. The NBC is imposed for the temporal direction, and the PBC for the spatial direction. In Table I, we list $(1/g^2, L/a)$ which are used in the present

TABLE I. The $(1/g^2, L/a)$ values that are used in the present calculation.

Set	$1/g^2$	L/a
A	2.0786	6, 7, 8, 9, 10, 11, 12
	2.1043	7, 8, 9, 10, 11, 12, 13, 14
	2.1275	8, 9, 10, 11, 12, 13, 14, 15, 16
	2.1625	10, 12, 14, 16, 18, 20
	2.1954	12, 14, 16, 18, 20, 22, 24
	2.2403	16, 18, 20, 22, 24, 26, 28, 30, 32
B	1.9637	6, 7, 8, 9, 10, 11, 12
	1.9875	7, 8, 9, 10, 11, 12, 13, 14
	2.0100	8, 9, 10, 11, 12, 13, 14, 15, 16
	2.0489	10, 12, 14, 16, 18, 20
	2.0794	12, 14, 16, 18, 20, 22, 24
	2.1260	16, 18, 20, 22, 24, 26, 28, 30, 32
C	1.8439	6, 7, 8, 9, 10, 11, 12
	1.8711	7, 8, 9, 10, 11, 12, 13, 14
	1.8947	8, 9, 10, 11, 12, 13, 14, 15, 16
	1.9319	10, 12, 14, 16, 18, 20
	1.9637	12, 14, 16, 18, 20, 22, 24
	2.0100	16, 18, 20, 22, 24, 26, 28, 30, 32
D	1.7276	6, 7, 8, 9, 10, 11, 12
	1.7553	7, 8, 9, 10, 11, 12, 13, 14
	1.7791	8, 9, 10, 11, 12, 13, 14, 15, 16
	1.8171	10, 12, 14, 16, 18, 20
	1.8497	12, 14, 16, 18, 20, 22, 24
	1.8965	16, 18, 20, 22, 24, 26, 28, 30, 32
E	1.6050	6, 7, 8, 9, 10, 11, 12
	1.6346	7, 8, 9, 10, 11, 12, 13, 14
	1.6589	8, 9, 10, 11, 12, 13, 14, 15, 16
	1.6982	10, 12, 14, 16, 18, 20
	1.7306	12, 14, 16, 18, 20, 22, 24
	1.7800	16, 18, 20, 22, 24, 26, 28, 30, 32

calculation. As we will mention in Sec. IV A, we classify them into five sets ("A," "B," "C," "D," and "E") depending on the value of the renormalized coupling. The heat bath algorithm is used to update $\boldsymbol{\phi}$ configurations, and even sites and odd sites are alternately updated. After a thermalization by 5000 sweeps, we calculate

$$G^{(i)}_{\mathrm{inv}}(t) = \frac{1}{L^2}\sum_{x_1,y_1} \boldsymbol{\phi}(t_{\mathrm{src}}, x_1)\cdot\boldsymbol{\phi}(t, y_1) \tag{25}$$

on the ith configuration at every 100 sweeps. We set $t_{\mathrm{src}}/a = L/a$. The total number of samples is 999 950 for each parameter set. The expectation value of Eq. (25) is nothing less than the $O(n)$-invariant two-point Green function.

B. Autocorrelation

We consider the autocorrelation function of $G^{(i)}_{\mathrm{inv}}(t)$,

$$A(j) \equiv \frac{1}{N}\sum_{i=1}^{N}[(G^{(i)}_{\mathrm{inv}}(t) - \langle G_{\mathrm{inv}}(t)\rangle_0)(G^{(i+j)}_{\mathrm{inv}}(t) - \langle G_{\mathrm{inv}}(t)\rangle_j)], \tag{26}$$

where the angled brackets denote the expectation value

$$\langle G_{\mathrm{inv}}(t)\rangle_j \equiv \frac{1}{N}\sum_{i=1}^{N} G^{(i+j)}_{\mathrm{inv}}(t). \tag{27}$$

The function $A(j)$ represents the correlation between $G^{(i)}_{\mathrm{inv}}(t)$'s separated by the j-time measurements. For a precise analysis, we introduce the integrated autocorrelation time,

$$\tau_{\mathrm{int}}(j) = \frac{1}{2} + \sum_{i=1}^{j}\frac{A(i)}{A(0)}. \tag{28}$$

$2\tau_{\mathrm{int}}(\infty)$ will indicate the separation where the measurements can be regarded to be independent.

In Fig. 1, we give $2\tau_{\mathrm{int}}(j)$ for some values of $(1/g^2, L/a)$. To guarantee a reliable analysis, $N \gg j$ is required, and we adopt $N = 100000$. The statistical error is evaluated using the single-eliminated jackknife method. The autocorrelation time becomes large near the continuum limit, and thus we show the data for $1/g^2$ that gives the smallest lattice spacing from the sets A and E. For each $(1/g^2, L/a)$, the situations with $(t - t_{\mathrm{src}})/a = 10$, 20, and 30 are shown. The data with large $(t - t_{\mathrm{src}})/a$ do not give a significant contribution to the evaluation of the mass gap and amplitude. We consider that the verification at $(t - t_{\mathrm{src}})/a = 10$–30 is sufficient. We confirm, from Fig. 1, that $2\tau_{\mathrm{int}}(\infty)$ is at most about 10 with our simulation parameters. For the sake of safety, we evaluate the statistical errors on the mass gap and amplitude by the jackknife method with a bin size of 50 samples in the following analysis.

C. Fit range

For the $O(N)$-invariant two-point Green function, we carry out the fit considering the correlation between the different time slices with the variance-covariance matrix. We denote the fit range as $[t_{\mathrm{min}} : t_{\mathrm{max}}]$. For all of the parameter sets, $(t_{\mathrm{max}} - t_{\mathrm{src}})/a = 3(L/a) - 1$ is chosen to avoid contamination from the temporal boundary. On the other hand, t_{min} should be determined from the behavior of χ^2/N_{df}. We increase t_{min} from 1, and adopt the value when χ^2/N_{df} falls to the vicinity of 1. An example for $(1/g^2, L/a) = (2.2403, 32)$ is shown in Fig. 2. For this parameter set,

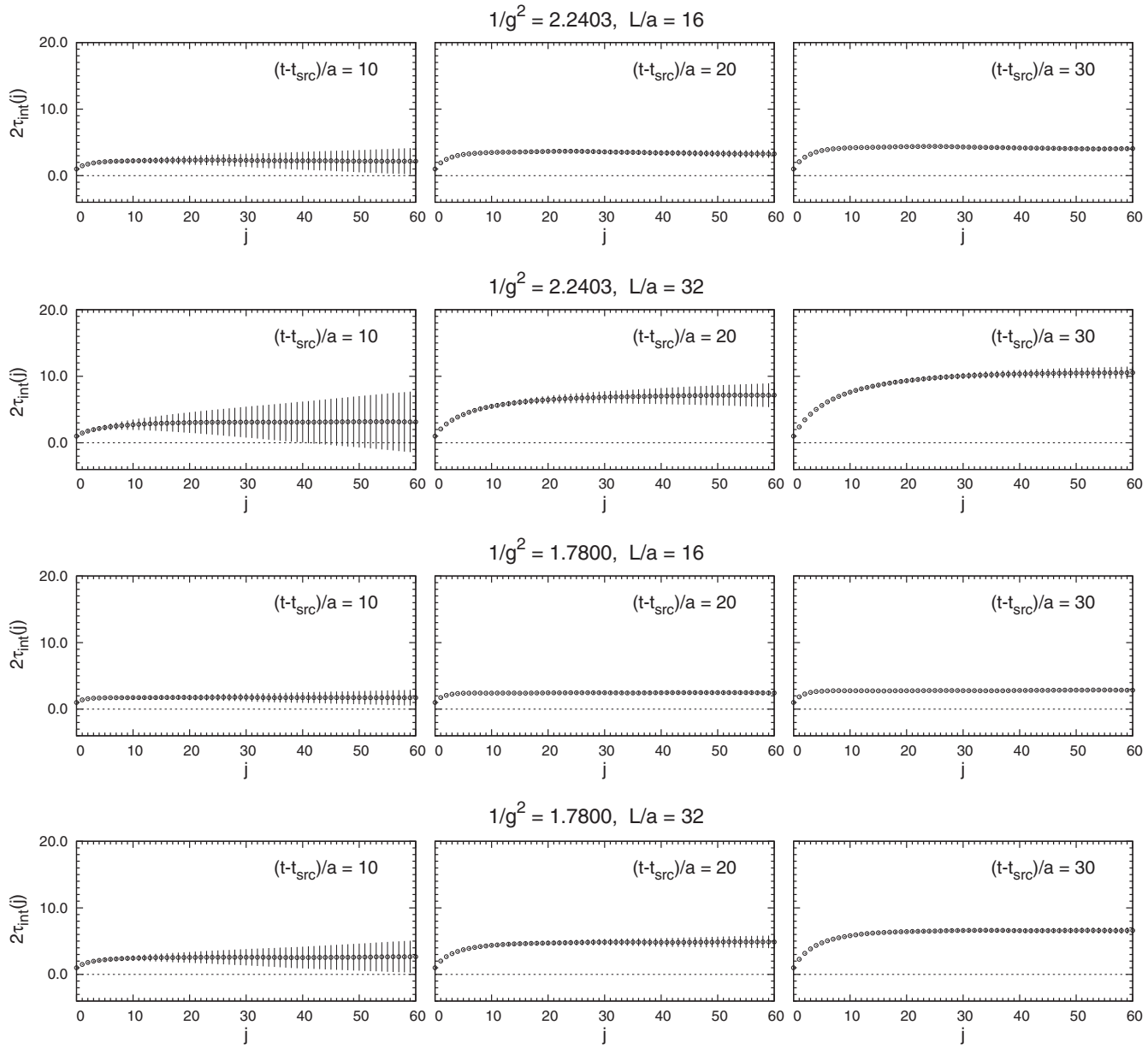

FIG. 1. $2\tau_{\rm int}(j)$ for some values of $(1/g^2, L/a)$. We show the data for $1/g^2$ that give the smallest lattice spacing from the sets A and E. For each $(1/g^2, L/a)$, the situations with $(t - t_{\rm src})/a = 10$, 20, and 30 are shown.

$(t_{\rm min} - t_{\rm src})/a = 12$ is adopted, and the fitted value is shown by the horizontal dotted lines.

IV. NUMERICAL RESULTS

A. Data of SSF

We obtain the mass gap in the lattice unit Ma and the amplitude A by fitting Eq. (6) to the data of the $O(n)$-invariant two-point Green function. The renormalized coupling $g^2_{\rm FV}$ can be extracted from Ma using Eq. (9), and the wave-function renormalization $Z^{\phi}_{\rm FV}$ from A using Eq. (10). On a lattice, $g^2_{\rm FV}$ and $Z^{\phi}_{\rm FV}$ depend on L/a in addition to the physical extent L. To take the continuum limit later, we classify the numerical data into five sets ("A," "B," "C," "D," and "E"). The classification is based on the value of $g^2_{\rm FV}$ in the smallest L for each $1/g^2$. We denote the smallest L as L_0. In Tables II–VI, we show $g^2_{\rm FV}(L, L/a)$ and $Z^{\phi}_{\rm FV}(L, L/a)$ measured with various $(1/g^2, L/a)$. We also list $\chi^2/N_{\rm df}$ in the fit.

We can determine SSFs by using Eqs. (15) and (16). However, they are the SSFs on a lattice. We need to extrapolate the lattice SSFs to the continuum ones. In preparation, in each set we line up $g^2_{\rm FV}(L_0, L_0/a)$ with the specific value. As an example, we consider the set A in

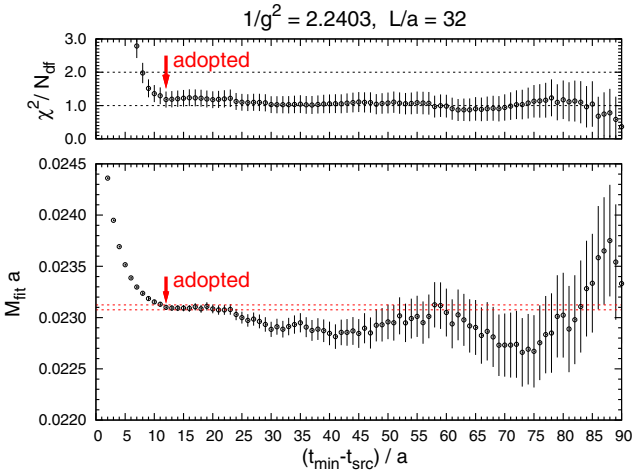

FIG. 2. An example of the fit-range dependence. $\chi^2/N_{\rm df}$ in the fit is shown in the top panel, and the fitted mass gap $M_{\rm fit}a$ is in the bottom panel. For this parameter set, $(t_{\rm min}-t_{\rm src})/a=12$ is adopted.

Table II. We adopt $u_0' \equiv 0.6755$ as the specific value. By using SSFs, we can evolve $g^2_{\rm FV}(L_0, L_0/a) = 0.6752$–$0.6756$ to $g^2_{\rm FV}(s_0 L_0, s_0 L_0/a) = u_0'$ with some factor s_0. In this situation, s_0 is nearly equal to 1, so we can safely use the perturbative expression for the continuum SSFs. By solving $u_0' = \sigma^g_{\rm P}(s_0, g^2_{\rm FV}(L_0, L_0/a))$ numerically with Newton's method, we determine s_0. Then, we evaluate the lattice SSFs by

$$\Sigma^g(s, u_0', a/L_0) = \sigma^g_{\rm P}(s_0, g^2_{\rm FV}(sL_0, sL_0/a)), \quad (29)$$

$$\Sigma^\phi(s, u_0', a/L_0) = \frac{\sigma^\phi_{\rm P}(s_0, g^2_{\rm FV}(sL_0, sL_0/a)) Z^\phi_{\rm FV}(sL_0, sL_0/a)}{\sigma^\phi_{\rm P}(s_0, g^2_{\rm FV}(L_0, L_0/a)) Z^\phi_{\rm FV}(L_0, L_0/a)}. \quad (30)$$

In the present study, $s \equiv L/L_0$ is a factor greater than 1 but not more than 2. The statistical errors are roughly estimated from

TABLE II. $g^2_{\rm FV}(L, L/a)$ and $Z^\phi_{\rm FV}(L, L/a)$ for various $(1/g^2, L/a)$ of set A.

$1/g^2 = 2.0786$				$1/g^2 = 2.1043$			
L/a	$g^2_{\rm FV}$	$Z^\phi_{\rm FV}$	$\chi^2/N_{\rm df}$	L/a	$g^2_{\rm FV}$	$Z^\phi_{\rm FV}$	$\chi^2/N_{\rm df}$
6	0.67562(44)	0.736987(89)	0.90(51)	7	0.67546(52)	0.71670(12)	0.83(45)
7	0.68841(53)	0.71269(12)	0.92(48)	8	0.68627(72)	0.69617(22)	1.92(67)
8	0.70089(50)	0.692435(98)	1.11(48)	9	0.69730(46)	0.678804(79)	1.06(44)
9	0.71109(47)	0.674314(80)	1.03(43)	10	0.70611(53)	0.66287(10)	1.00(41)
10	0.72053(54)	0.65817(10)	1.04(42)	11	0.71506(51)	0.648882(87)	1.38(45)
11	0.73019(52)	0.644050(89)	0.97(38)	12	0.72442(49)	0.636262(75)	0.81(33)
12	0.73917(59)	0.63109(11)	0.58(28)	13	0.73101(56)	0.624345(94)	0.85(33)
				14	0.73940(54)	0.613753(83)	0.98(33)
$1/g^2 = 2.1275$				$1/g^2 = 2.1625$			
L/a	$g^2_{\rm FV}$	$Z^\phi_{\rm FV}$	$\chi^2/N_{\rm df}$	L/a	$g^2_{\rm FV}$	$Z^\phi_{\rm FV}$	$\chi^2/N_{\rm df}$
8	0.67564(48)	0.700346(95)	1.30(52)	10	0.67532(50)	0.672916(98)	0.94(40)
9	0.68502(45)	0.682692(78)	1.18(46)	12	0.69241(47)	0.647087(74)	0.54(27)
10	0.69352(52)	0.66698(10)	1.08(42)	14	0.70607(51)	0.625249(80)	1.41(40)
11	0.70200(50)	0.653087(87)	1.63(49)	16	0.71807(48)	0.606667(65)	1.49(38)
12	0.71110(48)	0.640655(75)	0.59(28)	18	0.72879(61)	0.590271(93)	0.68(25)
13	0.71862(55)	0.629024(93)	1.09(37)	20	0.74184(51)	0.576403(61)	1.44(33)
14	0.72579(53)	0.618446(82)	1.01(34)				
15	0.73228(51)	0.608579(73)	0.96(32)				
16	0.73815(50)	0.599474(67)	1.29(36)				
$1/g^2 = 2.1954$				$1/g^2 = 2.2403$			
L/a	$g^2_{\rm FV}$	$Z^\phi_{\rm FV}$	$\chi^2/N_{\rm df}$	L/a	$g^2_{\rm FV}$	$Z^\phi_{\rm FV}$	$\chi^2/N_{\rm df}$
12	0.67551(46)	0.652903(72)	0.55(27)	16	0.67526(68)	0.62115(14)	1.11(34)
14	0.68986(43)	0.631629(58)	1.02(34)	18	0.68645(58)	0.605781(89)	0.65(24)
16	0.70072(47)	0.613205(64)	2.01(44)	20	0.69597(62)	0.591990(94)	0.99(28)
18	0.71007(60)	0.597037(92)	0.75(26)	22	0.70598(53)	0.579779(65)	1.25(30)
20	0.72075(64)	0.582953(96)	0.85(26)	24	0.71253(64)	0.568376(86)	1.08(27)
22	0.73000(62)	0.570317(82)	0.97(26)	26	0.71991(62)	0.558049(75)	0.90(23)
24	0.73715(74)	0.55872(11)	0.91(25)	28	0.72725(74)	0.548606(95)	0.82(22)
				30	0.73428(72)	0.539910(85)	1.17(25)
				32	0.73919(76)	0.531715(89)	1.18(24)

TABLE III. $g^2_{\rm FV}(L, L/a)$ and $Z^{\phi}_{\rm FV}(L, L/a)$ for various $(1/g^2, L/a)$ of set B.

$1/g^2 = 1.9637$				$1/g^2 = 1.9875$			
L/a	$g^2_{\rm FV}$	$Z^{\phi}_{\rm FV}$	$\chi^2/N_{\rm df}$	L/a	$g^2_{\rm FV}$	$Z^{\phi}_{\rm FV}$	$\chi^2/N_{\rm df}$
6	0.73747(63)	0.71909(17)	0.54(41)	7	0.73929(57)	0.69777(13)	1.12(53)
7	0.75339(58)	0.69344(13)	0.50(35)	8	0.75316(65)	0.67613(16)	0.96(46)
8	0.76891(55)	0.67183(10)	0.82(42)	9	0.76653(51)	0.657341(85)	1.56(53)
9	0.78230(52)	0.652625(87)	0.77(37)	10	0.77661(58)	0.64026(11)	0.80(36)
10	0.79236(71)	0.63504(16)	0.80(37)	11	0.78893(56)	0.625564(94)	0.77(34)
11	0.80587(57)	0.620335(95)	1.45(46)	12	0.79912(64)	0.61190(11)	0.79(33)
12	0.81642(66)	0.60642(12)	0.75(32)	13	0.80946(62)	0.59952(10)	1.05(36)
				14	0.81904(60)	0.588191(89)	0.97(33)
$1/g^2 = 2.0100$				$1/g^2 = 2.0489$			
L/a	$g^2_{\rm FV}$	$Z^{\phi}_{\rm FV}$	$\chi^2/N_{\rm df}$	L/a	$g^2_{\rm FV}$	$Z^{\phi}_{\rm FV}$	$\chi^2/N_{\rm df}$
8	0.74019(53)	0.68055(10)	1.29(52)	10	0.73761(66)	0.65247(15)	0.72(35)
9	0.75190(49)	0.661754(84)	0.79(38)	12	0.75740(60)	0.62503(11)	0.76(33)
10	0.76117(68)	0.64466(16)	0.58(32)	14	0.77468(57)	0.602081(86)	1.23(38)
11	0.77292(55)	0.630250(92)	1.07(40)	16	0.78772(80)	0.58195(15)	0.74(28)
12	0.78414(53)	0.616994(80)	0.80(33)	18	0.80339(68)	0.565226(98)	0.87(28)
13	0.79270(60)	0.604552(99)	0.82(32)	20	0.81694(73)	0.55012(10)	1.08(30)
14	0.80228(59)	0.593399(88)	1.30(39)				
15	0.80917(76)	0.58254(14)	0.98(33)				
16	0.81636(83)	0.57284(16)	1.30(37)				
$1/g^2 = 2.0794$				$1/g^2 = 2.1260$			
L/a	$g^2_{\rm FV}$	$Z^{\phi}_{\rm FV}$	$\chi^2/N_{\rm df}$	L/a	$g^2_{\rm FV}$	$Z^{\phi}_{\rm FV}$	$\chi^2/N_{\rm df}$
12	0.73826(59)	0.63119(11)	0.55(28)	16	0.73845(58)	0.599035(88)	1.00(32)
14	0.75515(55)	0.608666(84)	0.95(33)	18	0.75124(63)	0.582660(95)	1.05(31)
16	0.76813(78)	0.58894(15)	0.94(32)	20	0.76170(67)	0.567950(98)	0.93(27)
18	0.78243(66)	0.572381(96)	0.80(27)	22	0.77400(66)	0.555121(85)	1.25(30)
20	0.79442(71)	0.55745(10)	1.05(29)	24	0.78255(78)	0.54314(11)	0.94(25)
22	0.80650(69)	0.544151(87)	1.02(27)	26	0.79209(76)	0.532309(95)	1.01(25)
24	0.81634(81)	0.53195(11)	0.75(23)	28	0.80000(90)	0.52232(12)	1.10(25)
				30	0.80918(87)	0.51320(11)	0.86(21)
				32	0.81889(84)	0.505102(95)	0.83(20)

TABLE IV. $g^2_{\rm FV}(L, L/a)$ and $Z^{\phi}_{\rm FV}(L, L/a)$ for various $(1/g^2, L/a)$ of set C.

$1/g^2 = 1.8439$				$1/g^2 = 1.8711$			
L/a	$g^2_{\rm FV}$	$Z^{\phi}_{\rm FV}$	$\chi^2/N_{\rm df}$	L/a	$g^2_{\rm FV}$	$Z^{\phi}_{\rm FV}$	$\chi^2/N_{\rm df}$
6	0.81779(72)	0.69774(19)	0.59(42)	7	0.81674(80)	0.67550(23)	0.67(42)
7	0.8368(10)	0.66928(36)	1.30(61)	8	0.83601(60)	0.65282(11)	1.14(49)
8	0.85636(91)	0.64610(27)	1.09(51)	9	0.85232(57)	0.632517(92)	0.70(36)
9	0.87577(58)	0.626062(94)	1.01(43)	10	0.86582(78)	0.61411(17)	1.05(43)
10	0.89178(68)	0.60762(12)	0.95(40)	11	0.88066(75)	0.59823(14)	0.72(33)
11	0.90702(65)	0.59134(10)	1.12(41)	12	0.89595(72)	0.58385(12)	0.56(28)
12	0.92297(74)	0.57669(13)	0.93(36)	13	0.90939(70)	0.57061(11)	0.73(30)
				14	0.92210(68)	0.558491(97)	1.06(35)
$1/g^2 = 1.8947$				$1/g^2 = 1.9319$			
L/a	$g^2_{\rm FV}$	$Z^{\phi}_{\rm FV}$	$\chi^2/N_{\rm df}$	L/a	$g^2_{\rm FV}$	$Z^{\phi}_{\rm FV}$	$\chi^2/N_{\rm df}$
8	0.81744(59)	0.65790(11)	0.93(44)	10	0.81599(74)	0.62809(17)	1.10(44)
9	0.83262(55)	0.637830(91)	1.01(43)	12	0.84231(67)	0.59917(12)	0.72(32)

(Table continued)

TABLE IV. *(Continued)*

$1/g^2 = 1.8947$				$1/g^2 = 1.9319$			
L/a	g^2_{FV}	Z^{ϕ}_{FV}	χ^2/N_{df}	L/a	g^2_{FV}	Z^{ϕ}_{FV}	χ^2/N_{df}
10	0.84622(76)	0.61976(17)	0.84(38)	14	0.86368(73)	0.57445(12)	1.23(38)
11	0.86124(62)	0.60431(10)	1.22(43)	16	0.88138(89)	0.55311(16)	0.95(32)
12	0.87416(70)	0.58991(12)	0.81(33)	18	0.90137(76)	0.53532(11)	1.06(31)
13	0.88743(68)	0.57696(11)	1.15(38)	20	0.92031(82)	0.51936(11)	0.91(27)
14	0.89816(66)	0.564864(94)	1.02(34)				
15	0.90795(85)	0.55333(15)	1.00(33)				
16	0.91855(93)	0.54310(17)	0.86(30)				
$1/g^2 = 1.9637$				$1/g^2 = 2.0100$			
L/a	g^2_{FV}	Z^{ϕ}_{FV}	χ^2/N_{df}	L/a	g^2_{FV}	Z^{ϕ}_{FV}	χ^2/N_{df}
12	0.81642(66)	0.60642(12)	0.75(32)	16	0.81636(83)	0.57284(16)	1.30(37)
14	0.83773(61)	0.582484(90)	0.80(30)	18	0.83360(70)	0.55586(10)	0.76(26)
16	0.85333(86)	0.56138(16)	1.10(34)	20	0.84805(75)	0.54043(11)	0.82(26)
18	0.87205(73)	0.54388(10)	0.78(26)	22	0.86180(74)	0.526669(91)	1.21(29)
20	0.88871(80)	0.52819(11)	0.93(27)	24	0.87336(88)	0.51403(12)	1.00(26)
22	0.90454(77)	0.514099(93)	1.16(29)	26	0.88646(85)	0.50271(10)	0.95(24)
24	0.91761(93)	0.50112(12)	0.92(25)	28	0.8965(10)	0.49211(13)	1.17(26)
				30	0.90739(98)	0.48235(11)	0.87(21)
				32	0.92037(95)	0.47385(10)	0.92(21)

TABLE V. $g^2_{\mathrm{FV}}(L, L/a)$ and $Z^{\phi}_{\mathrm{FV}}(L, L/a)$ for various $(1/g^2, L/a)$ of set D.

$1/g^2 = 1.7276$				$1/g^2 = 1.7553$			
L/a	g^2_{FV}	Z^{ϕ}_{FV}	χ^2/N_{df}	L/a	g^2_{FV}	Z^{ϕ}_{FV}	χ^2/N_{df}
6	0.91813(82)	0.67343(21)	0.96(54)	7	0.91732(73)	0.65013(16)	1.76(66)
7	0.94527(76)	0.64314(16)	1.27(56)	8	0.94251(68)	0.62534(12)	0.88(43)
8	0.97343(71)	0.61815(13)	1.36(53)	9	0.96594(65)	0.60345(10)	1.01(43)
9	0.99753(66)	0.59562(10)	0.53(31)	10	0.98462(90)	0.58341(19)	0.99(42)
10	1.01974(78)	0.57552(13)	0.70(34)	11	1.00482(86)	0.56624(16)	1.17(42)
11	1.04285(76)	0.55802(11)	0.93(37)	12	1.02561(83)	0.55070(14)	0.92(36)
12	1.06385(86)	0.54171(14)	0.94(36)	13	0.10457(81)	0.53651(12)	0.84(32)
				14	1.06333(79)	0.52324(11)	1.90(47)
$1/g^2 = 1.7791$				$1/g^2 = 1.8171$			
L/a	g^2_{FV}	Z^{ϕ}_{FV}	χ^2/N_{df}	L/a	g^2_{FV}	Z^{ϕ}_{FV}	χ^2/N_{df}
8	0.91775(66)	0.63133(12)	1.10(48)	10	0.91626(83)	0.60044(18)	1.08(43)
9	0.93942(63)	0.609855(99)	0.89(40)	12	0.95094(77)	0.56913(13)	0.82(34)
10	0.95722(87)	0.59030(19)	1.00(42)	14	0.98082(97)	0.54265(18)	0.67(29)
11	0.97698(70)	0.57354(11)	0.97(38)	16	1.00748(80)	0.52021(11)	1.04(32)
12	0.99454(81)	0.55794(13)	0.84(34)	18	1.03295(88)	0.50068(11)	0.72(25)
13	1.01269(78)	0.54394(12)	1.15(38)	20	1.05874(95)	0.48347(12)	0.92(27)
14	1.02894(77)	0.53101(10)	1.38(40)				
15	1.04460(98)	0.51874(16)	1.07(34)				
16	1.05967(84)	0.50782(11)	1.00(32)				
$1/g^2 = 1.8497$				$1/g^2 = 1.8965$			
L/a	g^2_{FV}	Z^{ϕ}_{FV}	χ^2/N_{df}	L/a	g^2_{FV}	Z^{ϕ}_{FV}	χ^2/N_{df}
12	0.91781(74)	0.57834(13)	0.79(33)	16	0.91747(94)	0.54374(17)	1.39(38)
14	0.94411(69)	0.552425(97)	0.82(31)	18	0.93771(79)	0.52531(11)	0.85(28)

(Table continued)

TABLE V. *(Continued)*

$1/g^2 = 1.8497$				$1/g^2 = 1.8965$			
L/a	$g^2_{\rm FV}$	$Z^\phi_{\rm FV}$	$\chi^2/N_{\rm df}$	L/a	$g^2_{\rm FV}$	$Z^\phi_{\rm FV}$	$\chi^2/N_{\rm df}$
16	0.96708(99)	0.52991(18)	0.92(31)	20	0.95696(86)	0.50888(11)	1.23(31)
18	0.99091(83)	0.51113(11)	0.74(26)	22	0.97658(84)	0.494351(98)	1.14(29)
20	1.01343(91)	0.49428(12)	1.01(29)	24	0.9918(10)	0.48081(13)	0.88(24)
22	1.03716(89)	0.47935(10)	1.04(27)	26	1.00912(98)	0.46880(10)	1.03(25)
24	1.0539(11)	0.46540(13)	1.15(28)	28	1.0244(11)	0.45765(12)	0.90(23)
				30	1.0401(11)	0.44730(12)	1.05(24)
				32	1.0560(11)	0.43810(11)	1.47(27)

TABLE VI. $g^2_{\rm FV}(L, L/a)$ and $Z^\phi_{\rm FV}(L, L/a)$ for various $(1/g^2, L/a)$ of set E.

$1/g^2 = 1.6050$				$1/g^2 = 1.6346$			
L/a	$g^2_{\rm FV}$	$Z^\phi_{\rm FV}$	$\chi^2/N_{\rm df}$	L/a	$g^2_{\rm FV}$	$Z^\phi_{\rm FV}$	$\chi^2/N_{\rm df}$
6	1.05866(98)	0.64252(24)	1.58(70)	7	1.0574(11)	0.61760(29)	0.36(31)
7	1.10194(90)	0.60934(18)	1.16(54)	8	1.09602(81)	0.59098(14)	1.14(49)
8	1.14332(85)	0.58142(14)	1.78(61)	9	1.12986(76)	0.56664(11)	1.28(48)
9	1.18096(80)	0.55636(12)	0.64(34)	10	1.16218(90)	0.54500(15)	0.77(36)
10	1.21769(95)	0.53412(15)	1.12(43)	11	1.19398(87)	0.52598(13)	0.72(33)
11	1.2535(11)	0.51437(19)	0.72(33)	12	1.2261(10)	0.50844(16)	1.32(43)
12	1.2896(11)	0.49645(16)	1.37(44)	13	1.25752(99)	0.49268(14)	0.92(34)
				14	1.28756(97)	0.47814(12)	1.26(38)
$1/g^2 = 1.6589$				$1/g^2 = 1.6982$			
L/a	$g^2_{\rm FV}$	$Z^\phi_{\rm FV}$	$\chi^2/N_{\rm df}$	L/a	$g^2_{\rm FV}$	$Z^\phi_{\rm FV}$	$\chi^2/N_{\rm df}$
8	1.06073(78)	0.59846(13)	0.80(41)	10	1.05950(82)	0.56631(14)	0.78(36)
9	1.09148(73)	0.57462(11)	0.66(35)	12	1.10810(90)	0.53170(14)	1.42(44)
10	1.12050(87)	0.55344(14)	0.66(33)	14	1.15522(86)	0.50309(11)	0.65(27)
11	1.14998(84)	0.53491(12)	1.21(42)	16	1.19819(97)	0.47839(12)	1.19(35)
12	1.17791(97)	0.51778(15)	0.69(31)	18	1.2397(11)	0.45698(13)	0.91(29)
13	1.20647(94)	0.50241(13)	1.12(38)	20	1.2813(12)	1.43811(14)	0.90(27)
14	1.23363(92)	0.48817(12)	1.47(41)				
15	1.2582(12)	0.47455(19)	1.25(37)				
16	1.2810(14)	0.46181(22)	1.26(37)				
$1/g^2 = 1.7306$				$1/g^2 = 1.7800$			
L/a	$g^2_{\rm FV}$	$Z^\phi_{\rm FV}$	$\chi^2/N_{\rm df}$	L/a	$g^2_{\rm FV}$	$Z^\phi_{\rm FV}$	$\chi^2/N_{\rm df}$
12	1.05944(86)	0.54277(14)	0.86(35)	16	1.05797(84)	0.50805(11)	1.18(34)
14	1.10256(82)	0.51503(11)	0.84(31)	18	1.08760(93)	0.48799(12)	0.77(26)
16	1.1338(12)	0.48998(20)	0.70(27)	20	1.1172(10)	0.47038(13)	0.91(27)
18	1.1731(10)	0.46981(12)	1.09(31)	22	1.14777(87)	0.454904(84)	1.01(27)
20	1.2083(11)	0.45137(13)	0.99(28)	24	1.1707(12)	0.44014(14)	0.93(25)
22	1.2470(11)	0.43537(11)	0.75(23)	26	1.1976(12)	0.42709(12)	1.03(25)
24	1.2772(13)	0.42008(15)	0.92(25)	28	1.2213(13)	0.41507(13)	1.36(28)
				30	1.2472(12)	0.40391(11)	1.11(24)
				32	1.2712(13)	0.39383(12)	0.81(20)

TABLE VII. $\Sigma^g(s, u_0', a/L_0)$ and $\Sigma^\phi(s, u_0', a/L_0)$ for set A ($u_0' = 0.6755$).

$L_0/a = 6$			$L_0/a = 7$		
s	Σ^g	Σ^ϕ	s	Σ^g	Σ^ϕ
7/6	0.68829(75)	0.96704(20)	8/7	0.68631(95)	0.97135(35)
8/6	0.70076(73)	0.93956(18)	9/7	0.69735(78)	0.94712(20)
9/6	0.71095(71)	0.91498(17)	10/7	0.70616(82)	0.92488(22)
10/6	0.72039(76)	0.89308(19)	11/7	0.71512(80)	0.90537(21)
11/6	0.73004(75)	0.87392(18)	12/7	0.72447(79)	0.88776(20)
12/6	0.73902(80)	0.85634(20)	13/7	0.73106(84)	0.87113(22)
			14/7	0.73945(83)	0.85635(21)
$L_0/a = 7$			$L_0/a = 10$		
s	Σ^g	Σ^ϕ	s	Σ^g	Σ^ϕ
9/8	0.68488(73)	0.97480(17)	12/10	0.69260(77)	0.96161(18)
10/8	0.69337(78)	0.95236(20)	14/10	0.70628(80)	0.92914(19)
11/8	0.70185(76)	0.93253(18)	16/10	0.71828(78)	0.90152(18)
12/8	0.71094(75)	0.91479(17)	18/10	0.72900(86)	0.87715(21)
13/8	0.71847(80)	0.89818(19)	20/10	0.74207(80)	0.85653(19)
14/8	0.72562(78)	0.88308(19)			
15/8	0.73212(77)	0.86900(18)			
16/8	0.73799(76)	0.85600(18)			
$L_0/a = 12$			$L_0/a = 16$		
s	Σ^g	Σ^ϕ	s	Σ^g	Σ^ϕ
14/12	0.68985(70)	0.96742(14)	18/16	0.6867(10)	0.97525(26)
16/12	0.70071(73)	0.93920(15)	20/16	0.6962(10)	0.95304(27)
18/12	0.71007(81)	0.91444(18)	22/16	0.70624(98)	0.93337(25)
20/12	0.72074(84)	0.89286(19)	24/16	0.7128(10)	0.91501(26)
22/12	0.73000(83)	0.87351(18)	26/16	0.7202(10)	0.89838(26)
24/12	0.73714(92)	0.85574(21)	28/16	0.7275(11)	0.88317(28)
			30/16	0.7346(11)	0.86917(27)
			32/16	0.7395(11)	0.85597(28)

TABLE VIII. $\Sigma^g(s, u_0', a/L_0)$ and $\Sigma^\phi(s, u_0', a/L_0)$ for set B ($u_0' = 0.7383$).

$L_0/a = 6$			$L_0/a = 7$		
s	Σ^g	Σ^ϕ	s	Σ^g	Σ^ϕ
7/6	0.75426(98)	0.96428(30)	8/7	0.75214(96)	0.96903(29)
8/6	0.76981(96)	0.93420(28)	9/7	0.76547(86)	0.94215(22)
9/6	0.78323(94)	0.90746(26)	10/7	0.77552(91)	0.91770(24)
10/6	0.7933(11)	0.88298(33)	11/7	0.78780(90)	0.89666(23)
11/6	0.80687(97)	0.86251(28)	12/7	0.79796(95)	0.87710(25)
12/6	0.8175(10)	0.84313(30)	13/7	0.80826(93)	0.85938(24)
			14/7	0.81781(92)	0.84318(24)
$L_0/a = 8$			$L_0/a = 10$		
s	Σ^g	Σ^ϕ	s	Σ^g	Σ^ϕ
9/8	0.74995(81)	0.97245(19)	12/10	0.7581(10)	0.95790(28)
10/8	0.75916(94)	0.94738(27)	14/10	0.77545(99)	0.92270(26)
11/8	0.77085(85)	0.92627(20)	16/10	0.7885(11)	0.89182(33)
12/8	0.78200(84)	0.90685(19)	18/10	0.8042(11)	0.86616(28)
13/8	0.79052(88)	0.88861(21)	20/10	0.8178(11)	0.84299(29)
14/8	0.80004(87)	0.87227(20)			

(Table continued)

TABLE VIII. *(Continued)*

$L_0/a = 8$			$L_0/a = 10$		
s	Σ^g	Σ^ϕ	s	Σ^g	Σ^ϕ
15/8	0.80689(99)	0.85635(26)			
16/8	0.8140(11)	0.84212(28)			
$L_0/a = 12$			$L_0/a = 16$		
s	Σ^g	Σ^ϕ	s	Σ^g	Σ^ϕ
14/12	0.75519(91)	0.96431(21)	18/16	0.75109(95)	0.97267(21)
16/12	0.7682(11)	0.93305(29)	20/16	0.76155(97)	0.94812(22)
18/12	0.78247(98)	0.90682(23)	22/16	0.77384(97)	0.92671(21)
20/12	0.7945(10)	0.88316(24)	24/16	0.7824(11)	0.90672(24)
22/12	0.8065(10)	0.86210(23)	26/16	0.7919(10)	0.88863(22)
24/12	0.8164(11)	0.84277(26)	28/16	0.7998(11)	0.87196(26)
			30/16	0.8090(11)	0.85674(24)
			32/16	0.8187(11)	0.84323(24)

TABLE IX. $\Sigma^g(s, u_0', a/L_0)$ and $\Sigma^\phi(s, u_0', a/L_0)$ for set C ($u_0' = 0.8166$).

$L_0/a = 6$			$L_0/a = 7$		
s	Σ^g	Σ^ϕ	s	Σ^g	Σ^ϕ
7/6	0.8355(13)	0.95926(58)	8/7	0.8359(12)	0.96644(37)
8/6	0.8550(13)	0.92610(47)	9/7	0.8522(12)	0.93639(35)
9/6	0.8744(11)	0.89743(30)	10/7	0.8657(13)	0.90914(41)
10/6	0.8903(11)	0.87103(32)	11/7	0.8805(13)	0.88563(39)
11/6	0.9055(11)	0.84774(31)	12/7	0.8958(12)	0.86435(37)
12/6	0.9214(12)	0.82678(33)	13/7	0.9092(12)	0.84476(37)
			14/7	0.9219(12)	0.82682(36)
$L_0/a = 8$			$L_0/a = 10$		
s	Σ^g	Σ^ϕ	s	Σ^g	Σ^ϕ
9/8	0.83175(92)	0.96953(21)	12/10	0.8430(12)	0.95392(32)
10/8	0.8453(11)	0.94209(30)	14/10	0.8644(12)	0.91453(32)
11/8	0.86030(97)	0.91863(22)	16/10	0.8821(13)	0.88053(37)
12/8	0.8732(10)	0.89678(25)	18/10	0.9021(12)	0.85218(31)
13/8	0.8864(10)	0.87710(24)	20/10	0.9211(12)	0.82675(33)
14/8	0.89713(99)	0.85874(23)			
15/8	0.9069(11)	0.84123(29)			
16/8	0.9175(12)	0.82569(32)			
$L_0/a = 12$			$L_0/a = 16$		
s	Σ^g	Σ^ϕ	s	Σ^g	Σ^ϕ
14/12	0.8379(10)	0.96052(24)	18/16	0.8338(13)	0.97034(32)
16/12	0.8535(12)	0.92571(32)	20/16	0.8483(13)	0.94341(32)
18/12	0.8723(11)	0.89685(26)	22/16	0.8621(13)	0.91937(31)
20/12	0.8889(12)	0.87096(27)	24/16	0.8736(14)	0.89731(34)
22/12	0.9048(11)	0.84773(26)	26/16	0.8867(14)	0.87753(33)
24/12	0.9178(12)	0.82632(29)	28/16	0.8967(15)	0.85903(36)
			30/16	0.9077(14)	0.84198(35)
			32/16	0.9207(14)	0.82714(34)

TABLE X. $\Sigma^g(s, u_0', a/L_0)$ and $\Sigma^\phi(s, u_0', a/L_0)$ for set D ($u_0' = 0.9176$).

$L_0/a = 6$			$L_0/a = 7$		
s	Σ^g	Σ^ϕ	s	Σ^g	Σ^ϕ
7/6	0.9447(13)	0.95505(39)	8/7	0.9428(12)	0.96185(30)
8/6	0.9728(13)	0.91796(36)	9/7	0.9662(12)	0.92817(28)
9/6	0.9969(13)	0.88453(34)	10/7	0.9849(13)	0.89734(38)
10/6	1.0191(13)	0.85469(36)	11/7	1.0052(13)	0.87092(34)
11/6	1.0422(13)	0.82873(36)	12/7	1.0260(13)	0.84700(32)
12/6	1.0631(14)	0.80452(38)	13/7	1.0461(13)	0.82517(31)
			14/7	1.0637(12)	0.80476(30)
$L_0/a = 8$			$L_0/a = 10$		
s	Σ^g	Σ^ϕ	s	Σ^g	Σ^ϕ
9/8	0.9393(11)	0.96599(24)	12/10	0.9524(13)	0.94778(36)
10/8	0.9571(12)	0.93501(35)	14/10	0.9824(15)	0.90361(42)
11/8	0.9768(11)	0.90847(25)	16/10	1.0091(14)	0.86618(34)
12/8	0.9944(12)	0.88376(29)	18/10	1.0347(14)	0.83360(36)
13/8	1.0125(12)	0.86160(27)	20/10	1.0606(15)	0.80490(37)
14/8	1.0288(12)	0.84112(26)			
15/8	1.0444(13)	0.82170(33)			
16/8	1.0595(12)	0.80439(28)			
$L_0/a = 12$			$L_0/a = 16$		
s	Σ^g	Σ^ϕ	s	Σ^g	Σ^ϕ
14/12	0.9439(12)	0.95521(27)	18/16	0.9378(15)	0.96610(36)
16/12	0.9668(14)	0.91629(37)	20/16	0.9571(15)	0.93587(37)
18/12	0.9907(13)	0.88382(29)	22/16	0.9767(15)	0.90915(35)
20/12	1.0132(13)	0.85469(30)	24/16	0.9919(16)	0.88424(38)
22/12	1.0369(13)	0.82889(29)	26/16	1.0093(16)	0.86215(37)
24/12	1.0536(14)	0.80476(33)	28/16	1.0246(16)	0.84165(38)
			30/16	1.0403(17)	0.82261(39)
			32/16	1.0562(16)	0.80567(38)

TABLE XI. $\Sigma^g(s, u_0', a/L_0)$ and $\Sigma^\phi(s, u_0', a/L_0)$ for set E ($u_0' = 1.0595$).

$L_0/a = 6$			$L_0/a = 7$		
s	Σ^g	Σ^ϕ	s	Σ^g	Σ^ϕ
7/6	1.1029(16)	0.94831(46)	8/7	1.0983(17)	0.95677(51)
8/6	1.1443(16)	0.90480(42)	9/7	1.1323(17)	0.91727(48)
9/6	1.1820(16)	0.86577(41)	10/7	1.1648(18)	0.88216(50)
10/6	1.2188(17)	0.83113(44)	11/7	1.1968(17)	0.85129(49)
11/6	1.2548(18)	0.80037(48)	12/7	1.2291(18)	0.82282(51)
12/6	1.2909(17)	0.77243(46)	13/7	1.2607(18)	0.79723(50)
			14/7	1.2909(18)	0.77363(50)
$L_0/a = 8$			$L_0/a = 10$		
s	Σ^g	Σ^ϕ	s	Σ^g	Σ^ϕ
9/8	1.0902(13)	0.96023(29)	12/10	1.1081(15)	0.93888(35)
10/8	1.1191(14)	0.92487(32)	14/10	1.1552(14)	0.88836(31)
11/8	1.1485(14)	0.89396(30)	16/10	1.1982(15)	0.84474(33)
12/8	1.1764(14)	0.86538(34)	18/10	1.2397(16)	0.80695(35)

(Table continued)

TABLE XI. *(Continued)*

$L_0/a = 8$			$L_0/a = 10$		
s	Σ^g	Σ^ϕ	s	Σ^g	Σ^ϕ
13/8	1.2048(14)	0.83973(32)	20/10	1.2813(16)	0.77362(37)
14/8	1.2319(14)	0.81597(31)			
15/8	1.2564(16)	0.79323(40)			
16/8	1.2791(17)	0.77197(45)			
$L_0/a = 12$			$L_0/a = 16$		
s	Σ^g	Σ^ϕ	s	Σ^g	Σ^ϕ
14/12	1.1026(15)	0.94887(32)	18/16	1.0892(15)	0.96045(32)
16/12	1.1339(17)	0.90272(44)	20/16	1.1190(15)	0.92574(33)
18/12	1.1731(16)	0.86557(34)	22/16	1.1496(15)	0.89521(28)
20/12	1.2083(16)	0.83158(36)	24/16	1.1727(17)	0.86611(35)
22/12	1.2471(16)	0.80210(35)	26/16	1.1996(17)	0.84037(33)
24/12	1.2773(18)	0.77393(40)	28/16	1.2234(17)	0.81670(35)
			30/16	1.2494(17)	0.79469(34)
			32/16	1.2735(18)	0.77481(35)

$$\Delta(\Sigma^g(s,u_0',a/L_0)) = \sqrt{\left[\frac{\partial\sigma_{\rm P}^g(s,u_0')}{\partial u}\frac{\partial\sigma_{\rm P}^g(s_0,u_0)}{\partial u}\Delta(u_0)\right]^2 + \left[\frac{\partial\sigma_{\rm P}^g(s_0,u_1)}{\partial u}\Delta(u_1)\right]^2}, \tag{31}$$

$$\Delta(\Sigma^\phi(s,u_0',a/L_0)) = \sqrt{\left[\Delta\left(\frac{\sigma_{\rm P}^\phi(s_0,u_1)}{\sigma_{\rm P}^\phi(s_0,u_0)}\right)\frac{v_1}{v_0}\right]^2 + \left[\frac{\sigma_{\rm P}^\phi(s_0,u_1)}{\sigma_{\rm P}^\phi(s_0,u_0)}\Delta\left(\frac{v_1}{v_0}\right)\right]^2}. \tag{32}$$

The symbol Δ denotes the statistical error. We denote $g^2_{\rm FV}(L_0,L_0/a)$ as u_0, $g^2_{\rm FV}(sL_0,sL_0/a)$ as u_1, $Z^\phi_{\rm FV}(L_0,L_0/a)$ as v_0, and $Z^\phi_{\rm FV}(sL_0,sL_0/a)$ as v_1 to simplify the expressions. $\Delta(\sigma_{\rm P}^\phi(s_0,u_1)/\sigma_{\rm P}^\phi(s_0,u_0))$ is estimated from

$$\Delta\left(\frac{\sigma_{\rm P}^\phi(s_0,u_1)}{\sigma_{\rm P}^\phi(s_0,u_0)}\right) = \sqrt{[E\Delta(u_0)]^2 + \left[\frac{1}{\sigma_{\rm P}^\phi(s_0,u_0)}\frac{\partial\sigma_{\rm P}^\phi(s_0,u_1)}{\partial u}\Delta(u_1)\right]^2}, \tag{33}$$

where the coefficient E is defined as

$$E \equiv -\frac{\sigma_{\rm P}^\phi(s_0,u_1)}{\sigma_{\rm P}^\phi(s_0,u_0)^2}\frac{\partial\sigma_{\rm P}^\phi(s_0,u_0)}{\partial u} - \left(\frac{1}{\sigma_{\rm P}^\phi(s_0,u_0)}\frac{\partial\sigma_{\rm P}^\phi(s_0,u_1)}{\partial s} - \frac{\sigma_{\rm P}^\phi(s_0,u_1)}{\sigma_{\rm P}^\phi(s_0,u_0)^2}\frac{\partial\sigma_{\rm P}^\phi(s_0,u_0)}{\partial s}\right)\frac{\partial\sigma_{\rm P}^g(s_0,u_0)/\partial u}{\partial\sigma_{\rm P}^g(s_0,u_0)/\partial s}. \tag{34}$$

In Tables VII–XI, we give $\Sigma^g(s,u_0',a/L_0)$ and $\Sigma^\phi(s,u_0',a/L_0)$ for various $(L_0/a,s)$ of each set. Each set corresponds to $u_0' = 0.6755$ for set A, $u_0' = 0.7383$ for set B, $u_0' = 0.8166$ for set C, $u_0' = 0.9176$ for set D, and $u_0' = 1.0595$ for set E.

In Fig. 3, we show the s dependence of $\Sigma^g(s,u_0',a/L_0)$ and $\Sigma^\phi(s,u_0',a/L_0)$ for various $(u_0',L_0/a)$. While the data points of $\Sigma^\phi(s,u_0',a/L_0)$ are almost located on a single curve independent of L_0/a, the data points of $\Sigma^g(s,u_0',a/L_0)$ show a larger fluctuation. One reason for this is that the renormalized coupling $g^2_{\rm FV}$ is defined by multiplying L/a by the dimensionless mass gap Ma. As a result, the uncertainty of Ma due to the fit-range dependence is amplified in the value of $g^2_{\rm FV}$. However, $\Sigma^g(s,u_0',a/L_0)$ might have a (L_0/a) dependence beyond this uncertainty. In Sec. IV B, we discuss the (L_0/a) dependence of $\Sigma^g(s,u_0',a/L_0)$ and $\Sigma^\phi(s,u_0',a/L_0)$, and evaluate the values at $(s,a/L_0) = (2,0)$.

B. Continuum limit

The continuum limit is nothing less than the limit $a/L_0 \to 0$. We extract the values of $\Sigma^{g,\phi}(s,u_0',a/L_0)$ at $(s,a/L_0) = (2,0)$ by fitting for each u_0'. We use the following fitting forms:

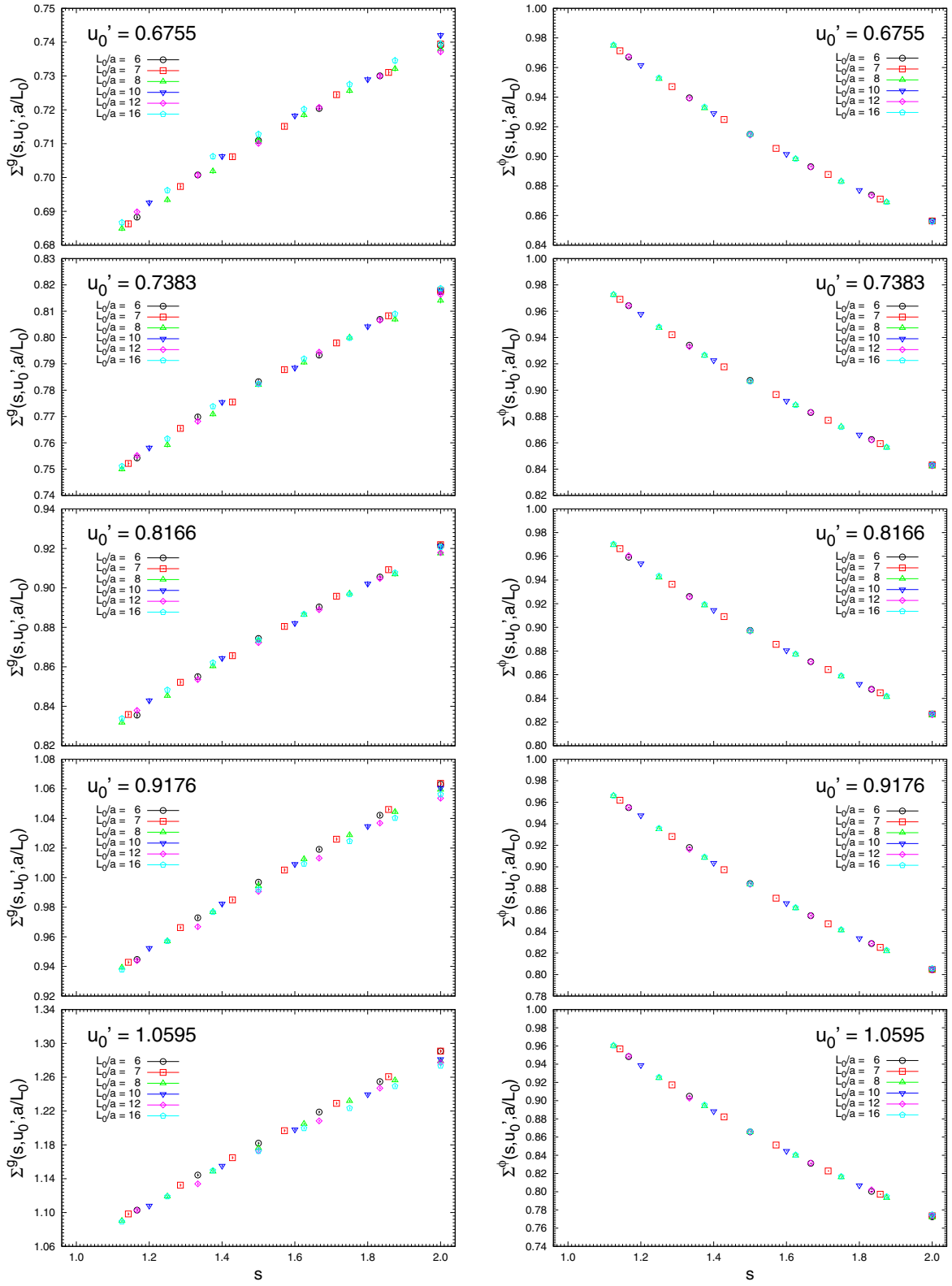

FIG. 3. s dependence of $\Sigma^g(s, u_0', a/L_0)$ and $\Sigma^\phi(s, u_0', a/L_0)$ for various $(u_0', L_0/a)$.

$$\Sigma^g(s,u_0',a/L_0) = u_0' + \sum_k W_k(s,a/L_0)\Sigma_k^g(u_0'), \quad (35)$$

$$\Sigma^\phi(s,u_0',a/L_0) = 1 + \sum_k W_k(s,a/L_0)\Sigma_k^\phi(u_0'). \quad (36)$$

The function $W_k(s,a/L_0)$ is defined by

$$W_{(i-1)j_{\max}+j}(s,a/L_0) \equiv (\ln s)^i (a/L_0)^{2j}, \quad (37)$$

for $i = 1,\ldots,i_{\max}$ and $j = 0,\ldots,j_{\max}-1$. These are motivated from Eqs. (20)–(22). $\Sigma_k^g(u_0')$ and $\Sigma_k^\phi(u_0')$ are free parameters. They are determined for each u_0' by minimizing χ^2, that is, by solving the linear simultaneous equation

$$\sum_l A_{kl}^{g,\phi}(u_0')\Sigma_l^{g,\phi}(u_0') = B_k^{g,\phi}(u_0'), \quad (38)$$

with

$$A_{kl}^{g,\phi}(u_0') \equiv \sum_{s,a/L_0} \frac{W_k(s,a/L_0)W_l(s,a/L_0)}{\Delta(\Sigma^{g,\phi}(s,u_0',a/L_0))^2}, \quad (39)$$

$$B_k^{g,\phi}(u_0') \equiv \sum_{s,a/L_0} \frac{(\bar{\Sigma}^{g,\phi}(s,u_0',a/L_0) - \{u_0',1\})W_k(s,a/L_0)}{\Delta(\Sigma^{g,\phi}(s,u_0',a/L_0))^2}. \quad (40)$$

Here $\bar{\Sigma}^{g,\phi}(s,u_0',a/L_0)$ denotes the expectation value of $\Sigma^{g,\phi}(s,u_0',a/L_0)$. $\{u_0',1\}$ means u_0' for $B_k^g(u_0')$, and 1 for $B_k^\phi(u_0')$. The summation is taken over $(s,a/L_0)$ used in the measurement.

We must pay special attention to the evaluation of the statistical errors of $\Sigma^{g,\phi}(s,u_0',0)$. When $(\ln s)$ takes a nonzero value, the correlation between the fitting parameters must be considered. The variance-covariance matrix for the parameter $\Sigma_k^{g,\phi}(u_0')$ can be described by $(A^{g,\phi}(u_0'))^{-1}$. Thus, the statistical errors are evaluated as

$$\Delta(\Sigma^{g,\phi}(s,u_0',0))^2 = \sum_{k,l}(A^{g,\phi}(u_0'))_{kl}^{-1}W_k(s,0)W_l(s,0). \quad (41)$$

Equations (17) and (18) suggest that we can evaluate the β function and the anomalous dimension at $\sigma^g(s,u_0') = \Sigma^g(s,u_0',0)$ with $\Sigma_k^{g,\phi}(u_0')$ determined by the fit. We evaluate the expectation values as

$$-s\frac{\partial\Sigma^g(s,u_0',0)}{\partial s} = -s\sum_k \frac{\partial W_k(s,0)}{\partial s}\Sigma_k^g(u_0'), \quad (42)$$

$$-s\frac{\partial \ln\Sigma^\phi(s,u_0',0)}{\partial s} = -\frac{s}{\Sigma^\phi(s,u_0',0)}\sum_k \frac{\partial W_k(s,0)}{\partial s}\Sigma_\phi^\phi(u_0'). \quad (43)$$

The statistical error of $-s\partial\Sigma^g(s,u_0',0)/\partial s$ is evaluated as

$$\Delta\left(-s\frac{\partial\Sigma^g(s,u_0',0)}{\partial s}\right)^2 = s^2\sum_{k,l}(A^g(u_0'))_{kl}^{-1}\frac{\partial W_k(s,0)}{\partial s}\frac{\partial W_l(s,0)}{\partial s}. \quad (44)$$

On the other hand, to evaluate the statistical error of $-s\partial\ln\Sigma^\phi(s,u_0',0)/\partial s$, we use the approximation $(\ln\Sigma^\phi)\simeq\Sigma^\phi-1$, and calculate

$$\Delta\left(-s\frac{\partial\ln\Sigma^\phi(s,u_0',0)}{\partial s}\right)^2 \simeq \left(-s\frac{\partial(\Sigma^\phi(s,u_0',0)-1)}{\partial s}\right)^2 = s^2\sum_{k,l}(A^\phi(u_0'))_{kl}^{-1} \times\frac{\partial W_k(s,0)}{\partial s}\frac{\partial W_l(s,0)}{\partial s}. \quad (45)$$

From Tables VII–XI, we find $|\Sigma^\phi-1|<0.23$ for $u_0' = 0.6755$–1.0595. To compensate for the underestimation due to the approximation, we multiply the evaluation of $\Delta(-s\partial\ln\Sigma^\phi(s,u_0',0)/\partial s)$ by the factor $1+0.23^2=1.0529$.

In Table XII, we give the fitting results for Eqs. (35) and (36) with $(i_{\max},j_{\max}) = (2,2)$. We show $\sigma^g(2,u_0') = \Sigma^g(2,u_0',0)$ and $\sigma^\phi(2,u_0') = \Sigma^\phi(2,u_0',0)$ for each u_0'. We also list the β function and the anomalous dimension at $\sigma^g(2,u_0') = \Sigma^g(2,u_0',0)$.

TABLE XII. The fitting results of Eqs. (35) and (36) with $(i_{\max},j_{\max}) = (2,2)$. We show $\sigma^g(2,u_0') = \Sigma^g(2,u_0',0)$ and $\sigma^\phi(2,u_0') = \Sigma^\phi(2,u_0',0)$ for each u_0'. We also list the β function and the anomalous dimension at $\sigma^g(2,u_0') = \Sigma^g(2,u_0',0)$.

u_0'	0.6755	0.7383	0.8166	0.9176	1.0595
$\chi^2/N_{\rm df}$ for Σ^g	1.57	1.20	1.15	1.33	1.60
$\chi^2/N_{\rm df}$ for Σ^ϕ	1.33	1.69	2.07	1.31	2.18
$\sigma^g(2,u_0')$	0.73932(59)	0.81688(68)	0.91793(83)	1.05414(95)	1.2716(11)
$\sigma^\phi(2,u_0')$	0.85580(14)	0.84272(16)	0.82635(21)	0.80520(23)	0.77470(24)
$\beta_{\rm FV}(\sigma^g(2,u_0'))$	−0.0939(37)	−0.1251(43)	−0.1595(53)	−0.2310(61)	−0.3741(69)
$\gamma_{\rm FV}(\sigma^g(2,u_0'))$	0.23698(93)	0.2593(11)	0.2943(14)	0.3342(16)	0.4031(16)

C. Scale dependence

We discuss the continuum SSFs with $s = 2$, which were obtained in the analysis of Sec. IV B. In Fig. 4, we give a comparison between the Monte Carlo simulations and the perturbative evaluation. $\sigma^g(2, g^2_{\rm FV})$ and $\sigma^\phi(2, g^2_{\rm FV})$ are shown in the top and bottom panels, respectively. It can be observed that the perturbative evaluation approaches the result from Monte Carlo simulations as the order increases. Moreover, we fit

$$\sigma^g_{\rm F}(2,u) \equiv u + u^2\left(\frac{n-2}{2\pi}(\ln 2)\right) + u^3\left(\frac{n-2}{4\pi^2}(\ln 2) + \frac{(n-2)^2}{4\pi^2}(\ln 2)^2\right) + \sum_{i=2}^{5} u^{i+2}\sigma^g_i, \tag{46}$$

$$\sigma^\phi_{\rm F}(2,u) \equiv 1 + u\left(-\frac{n-1}{2\pi}(\ln 2)\right) + \sum_{i=1}^{4} u^{i+1}\sigma^\phi_i \tag{47}$$

to the Monte Carlo data, where σ^g_i $(2 \le i \le 5)$ and σ^ϕ_i $(1 \le i \le 4)$ are free parameters in the fit. We use the universal forms independent of the renormalization scheme for the first three terms of $\sigma^g_{\rm F}(2, g^2_{\rm FV})$, and the first two terms of $\sigma^\phi_{\rm F}(2, g^2_{\rm FV})$. $\chi^2/N_{\rm df}$ in the fit is 0.40 for $\sigma^g(2, g^2_{\rm FV})$, and 0.024 for $\sigma^\phi(2, g^2_{\rm FV})$. The fitting result is also shown in Fig. 4.

We consider the scale dependence of $g^2_{\rm FV}$ and $Z^\phi_{\rm FV}$. The SSFs are determined by the fit to Eqs. (46) and (47), and are expected to be sufficiently precise in the range $g^2_{\rm FV} = 0.67$–1.27. With the SSFs, we determine $g^2_{\rm FV}(2^k L_{\rm min})$ and $Z^\phi_{\rm FV}(2^k L_{\rm min})$ $(k = 0, \ldots, 5)$ using Eqs. (15) and (16). Here $L_{\rm min}$ is defined by $L_{\rm min} = 2^{-5} L_{\rm max}$, with $mL_{\rm max} = 0.5557(13)$. m is the mass gap at infinite volume. The value of $mL_{\rm max}$ corresponds to $g^2_{\rm FV}(L_{\rm max}) = 1.2680$, and is taken from Ref. [2]. In addition, we set $Z^\phi_{\rm FV}(L_{\rm max}) = 1.0$. Note that the values of $g^2_{\rm FV}(L_{\rm max})$ and $Z^\phi_{\rm FV}(L_{\rm max})$ are set without statistical errors. The statistical errors of $g^2_{\rm FV}(L)$ and $Z^\phi_{\rm FV}(L)$ are recursively estimated by

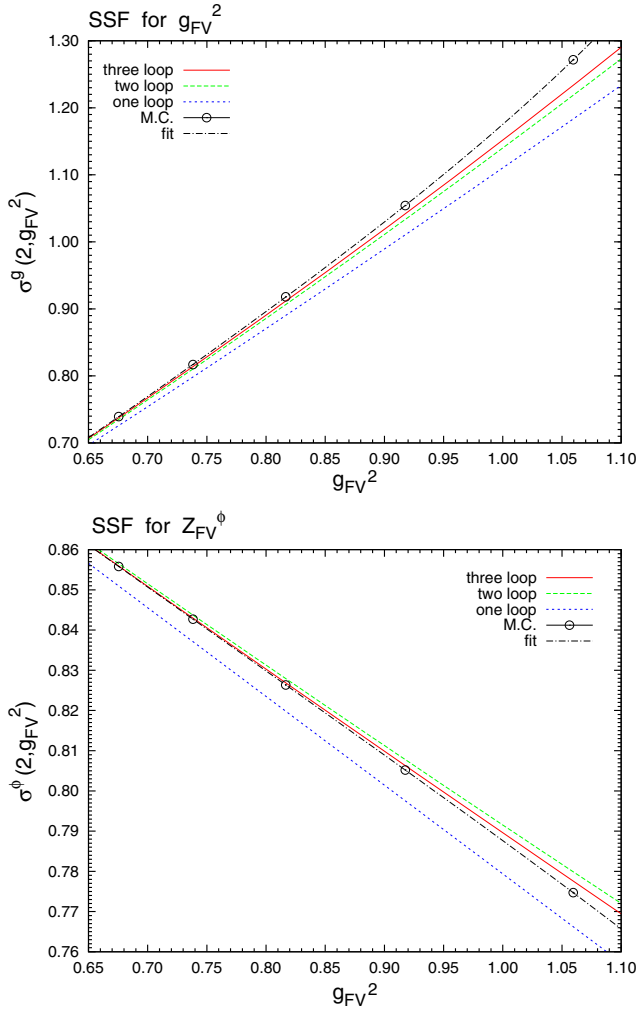

FIG. 4. SSFs obtained from Monte Carlo simulations and perturbative evaluation. $\sigma^g(2, g^2_{\rm FV})$ and $\sigma^\phi(2, g^2_{\rm FV})$ are shown in the top and bottom panels, respectively. The one-loop evaluation is described by the blue dotted curve, the two-loop one by the green dashed curve, and the three-loop one by the red solid curve. The result fitted to Eqs. (46) or (47) is given by the black dashed-dotted curve.

$$\Delta(g^2_{\rm FV}(L)) = \frac{1}{[\partial\sigma^g_{\rm F}(2,u)/\partial u]_{u=g^2_{\rm FV}(L)}}\sqrt{[\Delta(g^2_{\rm FV}(2L))]^2 + [\Delta(\sigma^g_{\rm F}(2, g^2_{\rm FV}(L)))]^2}, \tag{48}$$

$$\Delta(Z^\phi_{\rm FV}(L)) = \frac{1}{\sigma^\phi_{\rm F}(2, g^2_{\rm FV}(L))}\sqrt{[\Delta(Z^\phi_{\rm FV}(2L))]^2 + \left[\frac{\Delta(\sigma^\phi_{\rm F}(2, g^2_{\rm FV}(L)))}{\sigma^\phi_{\rm F}(2, g^2_{\rm FV}(L))} Z^\phi_{\rm FV}(2L)\right]^2}. \tag{49}$$

$\Delta(\sigma^{g,\phi}_{\rm F}(2, g^2_{\rm FV}(L)))$ denotes the statistical error due to those from the fitting parameters. For the estimation, we include a contribution from the correlation between the parameters, as we have done in Sec. IV B. In Table XIII, the values of $m \times 2^k L_{\rm min}$, $g^2_{\rm FV}(2^k L_{\rm min})$ and $Z^\phi_{\rm FV}(2^k L_{\rm min})$ $(k = 0, \ldots, 5)$ are listed. In Fig. 5, these data are plotted. We also show the results obtained by numerically integrating Eqs. (13) and (14) from $mL_{\rm min} = 0.017366$ with the perturbative $\beta_{\rm FV}(g^2_{\rm FV})$ and $\gamma_{\rm FV}(g^2_{\rm FV})$. We observe that the Monte Carlo data behaves reasonably in comparison with the perturbative evaluation.

Finally, we discuss the β function and the anomalous dimension. In principle, we can obtain them by differentiating $g^2_{\rm FV}(L)$ and $Z^\phi_{\rm FV}(L)$ with respect to L. However,

TABLE XIII. $g^2_{\rm FV}(2^k L_{\rm min})$ and $Z^{\phi}_{\rm FV}(2^k L_{\rm min})$ $(k = 0, \ldots, 5)$ determined with the SSFs by using Eqs. (15) and (16). We set $g^2_{\rm FV}(L_{\rm max}) = 1.2680$ and $Z^{\phi}_{\rm FV}(L_{\rm max}) = 1.0$ without statistical errors at $L_{\rm max} = 2^5 L_{\rm min}$. $g^2_{\rm FV}(L_{\rm max}) = 1.2680$ corresponds to $mL_{\rm max} = 0.5557(13)$.

k	$m \times 2^k L_{\rm min}$	$g^2_{\rm FV}(2^k L_{\rm min})$	$Z^{\phi}_{\rm FV}(2^k L_{\rm min})$
0	0.017366(41)	0.67548(76)	2.6916(13)
1	0.034731(81)	0.73917(74)	2.3035(11)
two	0.06946(16)	0.81829(80)	1.94076(87)
3	0.13893(33)	0.91982(81)	1.60311(66)
4	0.27785(65)	1.05738(63)	1.29005(39)
5	0.5557(13)	1.2680	1.0

the functional forms of $g^2_{\rm FV}(L)$ and $Z^{\phi}_{\rm FV}(L)$ are complicated, and thus performing the differentiation numerically seems to be difficult. We alternatively use the data for $\beta_{\rm FV}(\sigma^g(2, u_0'))$ and $\gamma_{\rm FV}(\sigma^g(2, u_0'))$ determined in Sec. IV B. In Fig. 6, the results from the Monte Carlo simulation are shown. The perturbative evaluation is also shown for comparison. We again observe reasonable behavior, although the statistical errors are relatively large compared to those of the SSFs or the renormalized parameters. It is possible to fit $\beta_{\rm FV}(g^2_{\rm FV})$ and $\gamma_{\rm FV}(g^2_{\rm FV})$ and determine the coefficients. However, we only have five data points in the present study. It is difficult to determine them with sufficient statistical precision, and thus we do not perform the fit. We leave the precise determination of the coefficients as a future task.

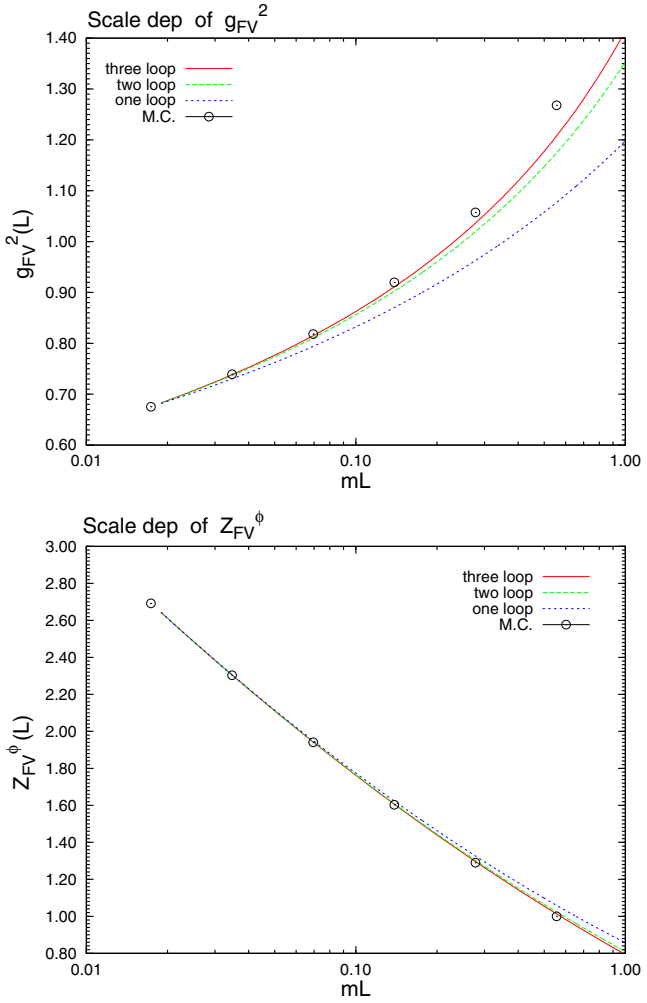

FIG. 5. Scale dependence of $g^2_{\rm FV}$ and $Z^{\phi}_{\rm FV}$. In addition to the results from Monte Carlo simulations, we also plot the results obtained by numerically integrating Eqs. (13) and (14) from $mL = 0.017366$ with the perturbative $\beta_{\rm FV}(g^2_{\rm FV})$ and $\gamma_{\rm FV}(g^2_{\rm FV})$. The one-loop evaluation is described by the blue dotted curve, the two-loop one by the green dashed curve, and the three-loop one by the red solid curve.

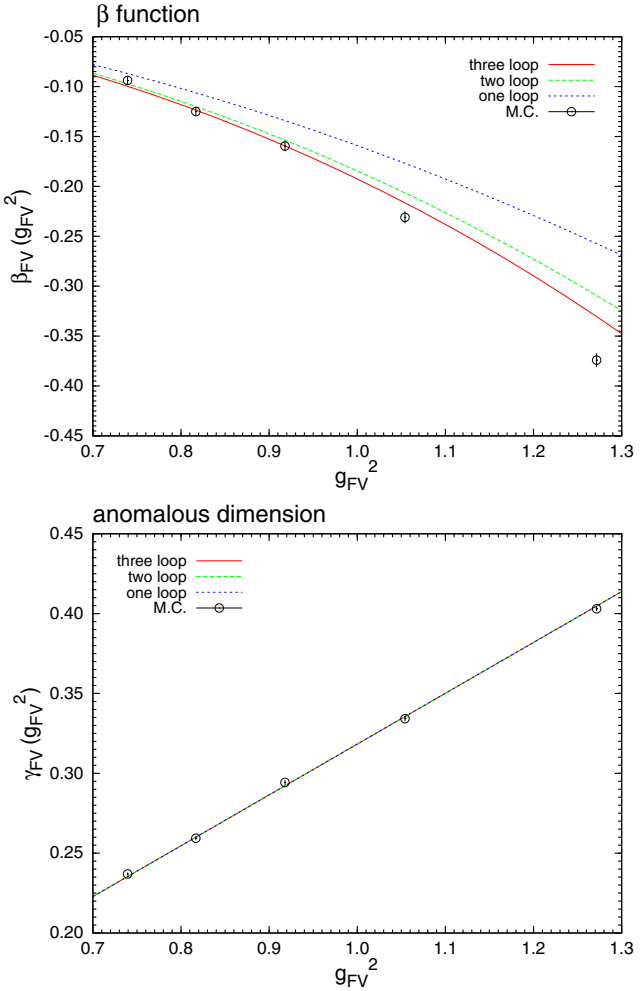

FIG. 6. $\beta_{\rm FV}(\sigma^g(2, u_0'))$ and $\gamma_{\rm FV}(\sigma^g(2, u_0'))$ determined in Sec. IV B. The former is shown in the top panel, and the latter in the bottom panel. The perturbative evaluation is also plotted for comparison. The one-loop evaluation is described by the blue dotted curve, the two-loop one by the green dashed curve, and the three-loop one by the red solid curve.

V. CONCLUSION

We have studied the finite box-size effects on the wave-function renormalization of the two-dimensional $O(3)$ sigma model. We have analyzed the SSF, which was proposed in a successful analysis of the renormalized coupling of the same model [2]. The SSF of the wave-function renormalization factor, Z^{ϕ}_{FV}, was determined with sufficient precision and its scale dependence was studied. We have compared the results with the perturbative evaluation and found a good agreement between them. The β function and the anomalous dimension were determined and it was found that their behaviors are also consistent with the perturbative evaluation.

Our analysis shows that the RG description of Z^{ϕ}_{FV} works well, and thus it gives further evidence for the existence of an RG equation that describes the box-size dependence of the N-point Green function. A concrete construction of the RG equation will be addressed in a forthcoming report [22].

To conclude, we give some prospective views. The RG equation in few-body quantum systems will be a useful tool for the analysis of spatially extended objects, such as (loosely) bound two- or few-body systems and the Efimov-like critical behaviors of the system, as we have mentioned in Sec. I. The analyses of the finite box-size effects should also have realistic physical meaning, as they are not artifacts or systematic errors. A well-known example is the finite-temperature system, where the finiteness in the imaginary time direction plays a key role. There the RG equation for the box-size parameter could be a new powerful tool for studying the temperature dependences.

ACKNOWLEDGMENTS

A part of the numerical calculations was carried out on the super parallel computers CRAY XC40 at YITP in Kyoto University.

APPENDIX: PERTURBATIVE EVALUATION

1. Preparation

To clarify the notation, we give a brief description of the action, Feynman rules, Green functions, and boundary condition.

We use dimensional regularization, so that Eq. (1) must be extended to a d-dimensional action,

$$S[\boldsymbol{\phi}] = \frac{1}{2g^2}\int_{\Lambda} d^d z \partial_\mu \boldsymbol{\phi}(z)\cdot\partial_\mu\boldsymbol{\phi}(z) \quad (\mu = 0,\ldots,d-1). \tag{A1}$$

Here the system is put on

$$\Lambda = \{z | z_0 \in [-T/2, T/2], z_i \in [0, L] \quad \text{for } i = 1,\ldots,d-1\}. \tag{A2}$$

As we have said in Sec. I, particular attention must be paid to the treatment of the zero mode. The zero mode comes from the degree of freedom where the $\boldsymbol{\phi}$ field is rotated by the same matrix over all points of space-time. To separate it, we use an $O(n)$ rotation matrix Ω which is independent of the space-time points, and parametrize the $\boldsymbol{\phi}$ field as

$$\boldsymbol{\phi}(z) = \Omega\left(\sqrt{1-g^2\boldsymbol{\pi}^2(z)}, g\boldsymbol{\pi}(z)\right)^T. \tag{A3}$$

$\boldsymbol{\pi}(z) = (\pi_i(z), i = 1,\ldots,n-1)$ is the $(n-1)$-component field. In the following, we use also the dot symbol for the scalar product of $(n-1)$-component vectors. As long as there is no confusion, we use the abbreviation, e.g., $\boldsymbol{\pi}^2 = \boldsymbol{\pi}\cdot\boldsymbol{\pi}$. According to Refs. [14,23], we consider the identity

$$1 = \int d^n \boldsymbol{m}\delta^n\left(\boldsymbol{m} - \frac{1}{TL^{d-1}}\int d^d z \boldsymbol{\phi}(z)\right). \tag{A4}$$

Substituting Eq. (A3) into Eq. (A4), we obtain

$$1 = S_{n-1}\left[\prod_{i=1}^{n-1}\delta\left(-\frac{g}{TL^{d-1}}\int d^d z \pi_i\right)\right] \times \exp\left[-\frac{(n-1)g^2}{2TL^{d-1}}\int d^d z \boldsymbol{\pi}^2\right], \tag{A5}$$

where S_{n-1} is the surface area of an $(n-1)$-dimensional unit sphere. Note that the identity (A5) is satisfied even in the interior of the path integration with respect to the $\boldsymbol{\pi}$ field. By applying Eq. (A5) to the partition function, we have

$$\begin{aligned}\mathcal{Z} &= \int [\delta(\boldsymbol{\phi}^2(z)-1)d\boldsymbol{\phi}(z)]\mathrm{e}^{-S[\boldsymbol{\phi}]} \\ &= \int\left[\frac{g d\boldsymbol{\pi}(z)}{\sqrt{1-g^2\boldsymbol{\pi}^2(z)}}\right]\exp\left[-\int d^d z\left\{\frac{1}{2}\partial_\mu\boldsymbol{\pi}\cdot\partial_\mu\boldsymbol{\pi} + \frac{g^2}{8}\frac{(\partial_\mu\boldsymbol{\pi}^2)^2}{1-g^2\boldsymbol{\pi}^2}\right\}\right] \\ &= \int [g d\boldsymbol{\pi}(z)]\exp\left[-\int d^d z\left\{\frac{1}{2}\partial_\mu\boldsymbol{\pi}\cdot\partial_\mu\boldsymbol{\pi} + \frac{g^2}{8}\frac{(\partial_\mu\boldsymbol{\pi}^2)^2}{1-g^2\boldsymbol{\pi}^2} + \frac{1}{2}\delta^d(0)\ln(1-g^2\boldsymbol{\pi}^2)\right\}\right]\end{aligned}$$

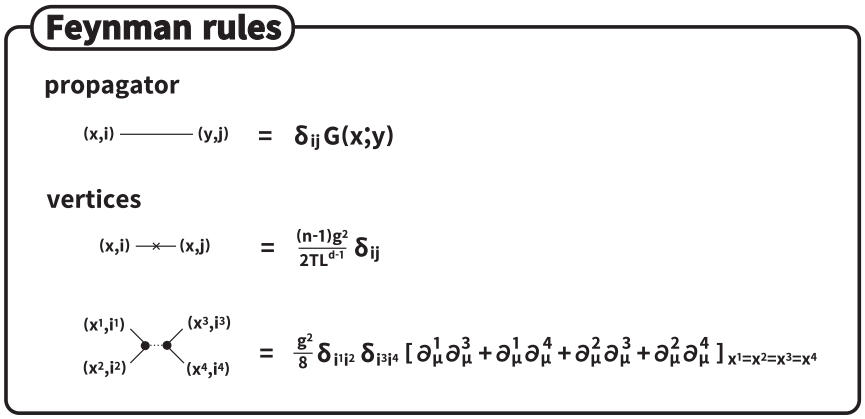

FIG. 7. Feynman rules read off from the action (A7) up to $\mathcal{O}(g^2)$. x and y represent the coordinates. i and j denote the number of components for the $\boldsymbol{\pi}$ field. The cross symbol denotes a vertex due to the zero mode. The filled circle denotes a vertex due to the term $\frac{g^2}{8}\frac{(\partial_\mu \boldsymbol{\pi}^2)^2}{1-g^2\boldsymbol{\pi}^2}$. Vertices linked by dotted lines are located at the same coordinate.

$$= S_{n-1}\int [gd\boldsymbol{\pi}(z)]\left[\prod_{i=1}^{n-1}\delta\left(-\frac{g}{TL^{d-1}}\int d^d z\pi_i\right)\right] \times \exp\left[-\int d^d z\left\{\frac{1}{2}\partial_\mu\boldsymbol{\pi}\cdot\partial_\mu\boldsymbol{\pi}+\frac{g^2}{8}\frac{(\partial_\mu\boldsymbol{\pi}^2)^2}{1-g^2\boldsymbol{\pi}^2}+\frac{1}{2}\delta^d(0)\ln(1-g^2\boldsymbol{\pi}^2)+\frac{(n-1)g^2}{2TL^{d-1}}\boldsymbol{\pi}^2\right\}\right]. \tag{A6}$$

The factor with the delta functions excludes the zero mode of the $\boldsymbol{\pi}$ field. To compensate, we must include an extra interaction term, $\frac{(n-1)g^2}{2TL^{d-1}}\boldsymbol{\pi}^2$.

Due to Eq. (A3), $\boldsymbol{\pi}$ must satisfy the condition $|\boldsymbol{\pi}| \le 1/g$. However, starting from the final expression of Eq. (A6), we are no longer constrained by the condition. It can also be understood from the free-field part of Eq. (A6) that $|\boldsymbol{\pi}| \le 1$ gives the main contribution to the path integration, and $|\boldsymbol{\pi}| \sim 1/g$ provides an exponentially small contribution. Thus, the range of integration can be safely extended to $|\boldsymbol{\pi}| < \infty$. See Ref. [24] for more details.

We have $\delta^d(0) = 0$ with the dimensional regularization.[1] Thus, we do not need to consider the interaction due to the integral measure, $\frac{1}{2}\delta^d(0)\ln(1-g^2\boldsymbol{\pi}^2)$, in the following discussion. Note that if we use lattice regularization, the IR cutoff mass g/a is introduced due to $\delta^2(0) = 1/a^2$ and enables us to isolate the momentum zero mode in a finite volume. The action for the $\boldsymbol{\pi}$ field can be written as

$$\begin{aligned} S[\boldsymbol{\pi}] &= \int d^d z\left[\frac{1}{2}\partial_\mu\boldsymbol{\pi}\cdot\partial^\mu\boldsymbol{\pi}+\frac{(n-1)g^2}{2TL^{d-1}}\boldsymbol{\pi}^2+\frac{g^2}{8}\frac{(\partial_\mu\boldsymbol{\pi}^2)^2}{1-g^2\boldsymbol{\pi}^2}\right] \\ &= \int d^d z\left[\frac{1}{2}\partial_\mu\boldsymbol{\pi}\cdot\partial^\mu\boldsymbol{\pi}+\frac{(n-1)g^2}{2TL^{d-1}}\boldsymbol{\pi}^2+\frac{g^2}{8}(\partial_\mu\boldsymbol{\pi}^2)^2+\mathcal{O}(g^4)\right]. \end{aligned} \tag{A7}$$

In Fig. 7, we summarize the Feynman rules that we can interpret from this action. The details of the $\boldsymbol{\pi}$ propagator, $G(x,y)$, are discussed a bit later.

[1]We can write $\delta^d(0) = \int_{-\infty}^{\infty}\frac{d^dk}{(2\pi)^d}1 = \int_{-\infty}^{\infty}\frac{d^dk}{(2\pi)^d}\frac{k^2+\alpha^2}{k^2+\alpha^2} = \int_{-\infty}^{\infty}\frac{d^dk}{(2\pi)^d}(k^2+\alpha^2)\int_0^\infty dt e^{-(k^2+\alpha^2)t}$ with an arbitrary nonzero parameter α. After changing the order of integration and doing the k integration, we have $\delta^d(0) = \frac{1}{2^d\pi^{d/2}}[\frac{d}{2}\int_0^\infty dt e^{-\alpha^2 t}t^{-d/2-1} + \alpha^2\int_0^\infty dt e^{-\alpha^2 t}t^{(-d/2+1)-1}]$. When $\mathrm{Re}(d) < 0$, these integrations converge, and we obtain $\delta^d(0) = 0$. Considering $\delta^d(0)$ as an analytical function of d, we can continue it to $\mathrm{Re}(d) \ge 0$. Then, we have $\delta^d(0) = 0$ for any complex dimension d.

We define the expectation value of an operator O as

$$\begin{aligned}\langle O\rangle &= \frac{S_{n-1}}{\mathcal{Z}}\int [gd\boldsymbol{\pi}(z)]\left[\prod_{i=1}^{n-1}\delta\left(-\frac{g}{TL^{d-1}}\int d^d z\pi_i\right)\right]\mathrm{e}^{-S_\pi}\times O \\ &= \frac{S_{n-1}}{\mathcal{Z}}\int [gd\boldsymbol{\pi}(z)]\left[\prod_{i=1}^{n-1}\delta\left(-\frac{g}{TL^{d-1}}\int d^d z\pi_i\right)\right] \\ &\times \mathrm{e}^{-\int d^d z\frac{1}{2}\partial_\mu\boldsymbol{\pi}\cdot\partial_\mu\boldsymbol{\pi}} O\left\{1-g^2\int d^d z\right. \\ &\left.\times\left[\frac{(n-1)}{2TL^{d-1}}\boldsymbol{\pi}^2+\frac{1}{8}(\partial_\mu\boldsymbol{\pi}^2)^2\right]+\mathcal{O}(g^4)\right\}. \end{aligned} \tag{A8}$$

In the following, the coefficient of $(g^2)^i$ is denoted by $\langle O\rangle_i$ with a non-negative integer i.

From Eq. (A8), the free $\boldsymbol{\pi}$ propagator,

$$\langle\pi_i(x)\pi_j(y)\rangle_0 = \delta_{ij}G(x;y), \tag{A9}$$

satisfies[2]

$$\Box_x G(x;y) = -\delta^d(x-y)+\frac{1}{TL^{d-1}}. \tag{A10}$$

To determine $G(x;y)$, the boundary condition must be set. We adopt the NBC for the temporal direction, and the PBC for the spatial direction,

$$\begin{aligned}&\frac{\partial}{\partial x_0}G(x_0,\boldsymbol{x};y_0,\boldsymbol{y}) = 0 \ \ (x_0=\pm T/2),\\ &\frac{\partial}{\partial y_0}G(x_0,\boldsymbol{x};y_0,\boldsymbol{y}) = 0 \ \ (y_0=\pm T/2),\\ &G(x_0,\boldsymbol{x}+L\boldsymbol{n}_x;y_0,\boldsymbol{y}+L\boldsymbol{n}_y) = G(x_0,\boldsymbol{x};y_0,\boldsymbol{y}) \ \ (\boldsymbol{n}_x,\boldsymbol{n}_y\in\mathbb{Z}^{d-1}).\end{aligned} \tag{A11}$$

Then, $G(x;y)$ can be written as

$$G(x;y) = \sum_{(m,\boldsymbol{n})\neq(0,\boldsymbol{0})}\frac{1}{\lambda^2_{m\boldsymbol{n}}}\phi^*_{m\boldsymbol{n}}(y)\phi_{m\boldsymbol{n}}(x), \tag{A12}$$

with

$$\lambda^2_{m\boldsymbol{n}} = p_m^2+\boldsymbol{q}_{\boldsymbol{n}}^2 \quad \left(p_m=\frac{\pi m}{T},\boldsymbol{q}_{\boldsymbol{n}}=\frac{2\pi\boldsymbol{n}}{L}\middle| m\in\mathbb{Z},\boldsymbol{n}\in\mathbb{Z}^{d-1}\right) \tag{A13}$$

and

$$\phi_{m\boldsymbol{n}}(x) = \begin{cases}\sqrt{1/(TL^{d-1})}\mathrm{e}^{i\boldsymbol{q}_{\boldsymbol{n}}\cdot\boldsymbol{x}} & (m=0),\\ \sqrt{2/(TL^{d-1})}\mathrm{e}^{i\boldsymbol{q}_{\boldsymbol{n}}\cdot\boldsymbol{x}}\cos(p_m x_0) & (m:\text{ even but not zero}),\\ \sqrt{2/(TL^{d-1})}\mathrm{e}^{i\boldsymbol{q}_{\boldsymbol{n}}\cdot\boldsymbol{x}}\sin(p_m x_0) & (m:\text{ odd}).\end{cases} \tag{A14}$$

$\lambda^2_{m\boldsymbol{n}}$ and $\phi_{m\boldsymbol{n}}(x)$ are the eigenvalue and eigenfunction of

$$\Box_x\phi(x) = -\lambda^2\phi(x) \tag{A15}$$

with the boundary condition

$$\begin{aligned}&\frac{\partial}{\partial x_0}\phi(x_0,\boldsymbol{x}) = 0 \qquad (x_0=\pm T/2),\\ &\phi(x_0,\boldsymbol{x}+L\boldsymbol{n}_x) = \phi(x_0,\boldsymbol{x}) \quad (\boldsymbol{n}_x\in\mathbb{Z}^{d-1}).\end{aligned} \tag{A16}$$

The normalization of $\varphi_{m\boldsymbol{n}}(x)$ is taken such that the orthonormal condition

$$\int_\Lambda d^d x\phi^*_{m\boldsymbol{n}}(x)\phi_{m'\boldsymbol{n}'}(x) = \delta_{mm'}\delta_{\boldsymbol{n}\boldsymbol{n}'} \tag{A17}$$

is satisfied.

It is useful to separate $G(x;y)$ as

$$G(x;y) = G_{\mathrm{Z}}(x_0;y_0)+G_{\mathrm{N}}(x;y), \tag{A18}$$

where $G_{\mathrm{Z}}(x_0;y_0)$ is a contribution from the momentum zero mode ($m\neq 0$, $\boldsymbol{n}=\boldsymbol{0}$),

$$G_{\mathrm{Z}}(x_0;y_0) \equiv \sum_{m\neq 0}\frac{1}{\lambda^2_{m\boldsymbol{0}}}\phi^*_{m\boldsymbol{0}}(y)\phi_{m\boldsymbol{0}}(x), \tag{A19}$$

and $G_{\mathrm{N}}(x;y)$ is the one from the momentum nonzero mode ($\boldsymbol{n}\neq\boldsymbol{0}$),

$$G_{\mathrm{N}}(x;y) \equiv \sum_m\sum_{\boldsymbol{n}\neq\boldsymbol{0}}\frac{1}{\lambda^2_{m\boldsymbol{n}}}\phi^*_{m\boldsymbol{n}}(y)\phi_{m\boldsymbol{n}}(x). \tag{A20}$$

After some calculations, we obtain

[2]The constant term, $\frac{1}{TL^{d-1}}$, appears due to the exclusion of the zero mode. Consider a formal solution $\tilde{G}(z)=\frac{1}{TL^{d-1}}\sum_{p\neq 0}\frac{\mathrm{e}^{ip\cdot z}}{p^2}$. One can confirm the appearance of the constant term from the calculation of $\Box_z\tilde{G}(z)=\frac{1}{TL^{d-1}}\sum_{p\neq 0}\frac{\Box_z\mathrm{e}^{ip\cdot z}}{p^2}=-\frac{1}{TL^{d-1}}\sum_p\mathrm{e}^{ip\cdot z}+\frac{1}{TL^{d-1}}\sum_{p=0}\mathrm{e}^{ip\cdot z}=-\delta^d(z)+\frac{1}{TL^{d-1}}$.

$$G_{\rm Z}(x_0;y_0)=\frac{1}{L^{d-1}}\left(-\frac{|x_0-y_0|}{2}+\frac{x_0^2+y_0^2}{2T}+\frac{T}{12}\right), \quad \text{(A21)}$$

$$G_{\rm N}(x;y)=\sum_{m=-\infty}^{\infty}\{R(x_0-y_0+2mT,\boldsymbol{x}-\boldsymbol{y}) + R(x_0+y_0+(2m+1)T,\boldsymbol{x}-\boldsymbol{y})\}, \quad \text{(A22)}$$

with the nonzero mode propagator in the limit of infinite temporal extent

$$R(z)\equiv\frac{1}{2L^{d-1}}\sum_{\boldsymbol{q}_n\neq\boldsymbol{0}}\frac{1}{|\boldsymbol{q}_n|}\mathrm{e}^{-|\boldsymbol{q}_n||z_0|+i\boldsymbol{q}_n\cdot\boldsymbol{z}}. \quad \text{(A23)}$$

Equation (A22) can be interpreted that $R(z)$ is padded in the temporal extent T in such a way as to satisfy the NBC. In addition, if we use the zero-mode propagator in the limit of infinite temporal extent,

$$r(z_0)=\frac{1}{2L^{d-1}}\lim_{\omega\to0^+}\frac{1}{\omega}\mathrm{e}^{-\omega|z_0|}, \quad \text{(A24)}$$

instead of $R(z)$ in Eq. (A22), we can reproduce Eq. (A21).

The $O(n)$-invariant two-point Green function defined by Eq. (4) can be written as

$$\begin{aligned}G_{\rm inv}(x;y)&=1+g^2\left(\langle\boldsymbol{\pi}(x)\cdot\boldsymbol{\pi}(y)\rangle-\frac{1}{2}\langle\boldsymbol{\pi}^2(x)\rangle-\frac{1}{2}\langle\boldsymbol{\pi}^2(y)\rangle\right)+g^4\left(\frac{1}{4}\langle\boldsymbol{\pi}^2(x)\boldsymbol{\pi}^2(y)\rangle-\frac{1}{8}\langle\boldsymbol{\pi}^4(x)\rangle-\frac{1}{8}\langle\boldsymbol{\pi}^4(y)\rangle\right)+\mathcal{O}(g^6)\\&=1+g^2\left(\langle\boldsymbol{\pi}(x)\cdot\boldsymbol{\pi}(y)\rangle_0-\frac{1}{2}\langle\boldsymbol{\pi}^2(x)\rangle_0-\frac{1}{2}\langle\boldsymbol{\pi}^2(y)\rangle_0\right)+g^4\left(\langle\boldsymbol{\pi}(x)\cdot\boldsymbol{\pi}(y)\rangle_1-\frac{1}{2}\langle\boldsymbol{\pi}^2(x)\rangle_1-\frac{1}{2}\langle\boldsymbol{\pi}^2(y)\rangle_1\right.\\&\quad\left.+\frac{1}{4}\langle\boldsymbol{\pi}^2(x)\boldsymbol{\pi}^2(y)\rangle_0-\frac{1}{8}\langle\boldsymbol{\pi}^4(x)\rangle_0-\frac{1}{8}\langle\boldsymbol{\pi}^4(y)\rangle_0\right)+\mathcal{O}(g^6). \quad \text{(A25)}\end{aligned}$$

The final expression of Eq. (A25) is perturbatively evaluated in Secs. A 2 and A 3.

2. Evaluation at $\mathcal{O}(g^2)$

It is instructive to follow the derivation of the $\mathcal{O}(g^2)$ contribution to the $O(n)$-invariant two-point Green function. The contribution is given by the second term in Eq. (A25). We refer to the contributions $\langle\boldsymbol{\pi}(x)\cdot\boldsymbol{\pi}(y)\rangle_0$, $\langle\boldsymbol{\pi}^2(x)\rangle_0$, and $\langle\boldsymbol{\pi}^2(y)\rangle_0$ as "a," "b," and "c," respectively. The diagrammatic description is given in Fig. 8. We project the total momentum in the external line to zero. Each contribution can be calculated as

$$\begin{aligned}P_{\rm a}(\tau)&=\frac{1}{L^{2(d-1)}}\int d^{d-1}\boldsymbol{x}\int d^{d-1}\boldsymbol{y}G(x;y)|_{x_0=-\tau,y_0=+\tau},\\P_{\rm b}(\tau)&=\frac{1}{L^{2(d-1)}}\int d^{d-1}\boldsymbol{x}\int d^{d-1}\boldsymbol{y}G(x;x)|_{x_0=-\tau},\\P_{\rm c}(\tau)&=\frac{1}{L^{2(d-1)}}\int d^{d-1}\boldsymbol{x}\int d^{d-1}\boldsymbol{y}G(y;y)|_{y_0=+\tau}, \quad \text{(A26)}\end{aligned}$$

except for the coefficient in Eq. (A25), the coefficient in the brackets of Eq. (A8), the multiplicity of the spin component, and the statistical factor. Here we adopt $x_0=-\tau$ and $y_0=+\tau$.

We do not need to consider the momentum nonzero mode for $P_{\rm a}(\tau)$,

$$P_{\rm a}(\tau)=G_{\rm Z}(x_0;y_0)|_{x_0=-\tau,y_0=+\tau}=\frac{1}{L^{d-1}}\left(-|\tau|+\frac{\tau^2}{T}+\frac{T}{12}\right). \quad \text{(A27)}$$

On the other hand, the momentum nonzero mode is needed for $P_{\rm b}(\tau)$ and $P_{\rm c}(\tau)$. Dropping the terms that are exponentially small for $T\to\infty$, we have

$$\begin{aligned}P_{\rm b}(\tau)&=G_{\rm Z}(x_0;x_0)|_{x_0=-\tau}+G_{\rm N}(x;x)|_{x_0=-\tau}\\&=\frac{1}{L^{d-1}}\left(\frac{\tau^2}{T}+\frac{T}{12}\right)+R(0), \quad \text{(A28)}\end{aligned}$$

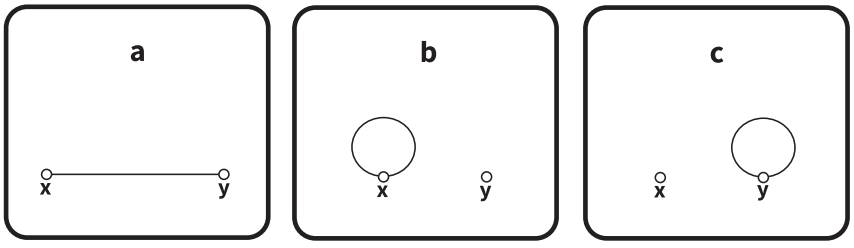

FIG. 8. The diagrammatic description of the $O(n)$-invariant two-point Green function at $\mathcal{O}(g^2)$. The open circle denotes the external space-time point.

$$P_{\rm c}(\tau) = G_{\rm Z}(y_0;y_0)|_{y_0=+\tau} + G_{\rm N}(y;y)|_{y_0=+\tau} = \frac{1}{L^{d-1}}\left(\frac{\tau^2}{T}+\frac{T}{12}\right) + R(0). \tag{A29}$$

In the derivation of Eqs. (A28) and (A29), the condition $-T/2 < \tau < T/2$ was used.

The factors multiplying each $P(\tau)$ are given by

$$F_{\rm a} = g^2 \times 1 \times (n-1) \times 1,$$
$$F_{\rm b} = (-g^2/2) \times 1 \times (n-1) \times 1,$$
$$F_{\rm c} = (-g^2/2) \times 1 \times (n-1) \times 1. \tag{A30}$$

Thus, the total contribution at $\mathcal{O}(g^2)$ can be written as

$$g^2 \frac{1}{L^{2(d-1)}} \int d^{d-1}\boldsymbol{x} \int d^{d-1}\boldsymbol{y} \langle \boldsymbol{\phi}(x)\cdot\boldsymbol{\phi}(y)\rangle_1 = F_{\rm a}P_{\rm a}(\tau) + F_{\rm b}P_{\rm b}(\tau) + F_{\rm c}P_{\rm c}(\tau) = g^2\left[-(n-1)R(0) - (n-1)\left(\frac{|\tau|}{L^{d-1}}\right)\right]. \tag{A31}$$

Note that the terms proportional to T cancel. This fact means that the divergence at $T\to\infty$ (IR divergence) vanishes by treating the $O(n)$-invariant Green function. It should also be noted that the terms proportional to τ^2 cancel. The appearance of the τ^2 terms in $P_{\rm b}(\tau)$ and $P_{\rm c}(\tau)$ is due to the use of the NBC. Such a cancellation does not occur if we use the periodic boundary condition for the temporal direction.

3. Evaluation at $\mathcal{O}(g^4)$

The $\mathcal{O}(g^4)$ contribution to the $O(n)$-invariant two-point Green function is given by the third term in Eq. (A25). We refer to the contributions $\langle\boldsymbol{\pi}(x)\cdot\boldsymbol{\pi}(y)\rangle_1$, $\langle\boldsymbol{\pi}^2(x)\rangle_1$, $\langle\boldsymbol{\pi}^2(y)\rangle_1$, $\langle\boldsymbol{\pi}^2(x)\boldsymbol{\pi}^2(y)\rangle_0$, $\langle\boldsymbol{\pi}^4(x)\rangle_0$, and $\langle\boldsymbol{\pi}^4(y)\rangle_0$ as "a," "b," "c," "d," "e," and "f," respectively. Moreover, we subdivide each contribution into groups based on the type of interaction or the pattern of contraction. The diagrammatic description is shown in Fig. 9. We again project the total momentum in the external line to zero, and introduce the abridged notation

$$\mathrm{Int}_2[f(x,y)] \equiv \frac{1}{L^{2(d-1)}}\int d^{d-1}\boldsymbol{x}\int d^{d-1}\boldsymbol{y}\,[f(x,y)]_{x_0=-\tau,y_0=+\tau},$$
$$\mathrm{Int}_3[f(x,y,z)] \equiv \frac{1}{L^{2(d-1)}}\int d^{d-1}\boldsymbol{x}\int d^{d-1}\boldsymbol{y}\int d^{d}z\,[f(x,y,z)]_{x_0=-\tau,y_0=+\tau}. \tag{A32}$$

Then, each contribution can be calculated as

$$\begin{aligned}
P_{\rm a0}(\tau) &= \mathrm{Int}_3[\partial_\mu^2 G(x;z)G(z;y)\partial_\mu^1 G(z;z) + \partial_\mu^2 G(x;z)G(z;y)\partial_\mu^2 G(z;z) + G(x;z)\partial_\mu^1 G(z;y)\partial_\mu^1 G(z;z) + G(x;z)\partial_\mu^1 G(z;y)\partial_\mu^2 G(z;z)],\\
P_{\rm a1}(\tau) &= \mathrm{Int}_3[\partial_\mu^2 G(x;z)G(z;y)\partial_\mu^2 G(z;z) + \partial_\mu^2 G(x;z)\partial_\mu^1 G(z;y)G(z;z) + G(x;z)G(z;y)\partial_\mu^1\partial_\mu^2 G(z;z) + G(x;z)\partial_\mu^1 G(z;y)\partial_\mu^1 G(z;z)],\\
P_{\rm a2}(\tau) &= \mathrm{Int}_3[G(x;z)G(z;y)],\\
P_{\rm b0}(\tau) &= \mathrm{Int}_3[\partial_\mu^2 G(x;z)G(z;x)\partial_\mu^1 G(z;z) + \partial_\mu^2 G(x;z)G(z;x)\partial_\mu^2 G(z;z) + G(x;z)\partial_\mu^1 G(z;x)\partial_\mu^1 G(z;z) + G(x;z)\partial_\mu^1 G(z;x)\partial_\mu^2 G(z;z)],\\
P_{\rm b1}(\tau) &= \mathrm{Int}_3[\partial_\mu^2 G(x;z)G(z;x)\partial_\mu^2 G(z;z) + \partial_\mu^2 G(x;z)\partial_\mu^1 G(z;x)G(z;z) + G(x;z)G(z;x)\partial_\mu^1\partial_\mu^2 G(z;z) + G(x;z)\partial_\mu^1 G(z;x)\partial_\mu^1 G(z;z)],\\
P_{\rm b2}(\tau) &= \mathrm{Int}_3[G(x;z)G(z;x)],\\
P_{\rm c0}(\tau) &= \mathrm{Int}_3[\partial_\mu^2 G(y;z)G(z;y)\partial_\mu^1 G(z;z) + \partial_\mu^2 G(y;z)G(z;y)\partial_\mu^2 G(z;z) + G(y;z)\partial_\mu^1 G(z;y)\partial_\mu^1 G(z;z) + G(y;z)\partial_\mu^1 G(z;y)\partial_\mu^2 G(z;z)],\\
P_{\rm c1}(\tau) &= \mathrm{Int}_3[\partial_\mu^2 G(y;z)G(z;y)\partial_\mu^2 G(z;z) + \partial_\mu^2 G(y;z)\partial_\mu^1 G(z;y)G(z;z) + G(y;z)G(z;y)\partial_\mu^1\partial_\mu^2 G(z;z) + G(y;z)\partial_\mu^1 G(z;y)\partial_\mu^1 G(z;z)],\\
P_{\rm c2}(\tau) &= \mathrm{Int}_3[G(y;z)G(z;y)],\\
P_{\rm d0}(\tau) &= \mathrm{Int}_2[G(x;x)G(y;y)],\\
P_{\rm d1}(\tau) &= \mathrm{Int}_2[G(x;y)G(x;y)],\\
P_{\rm e0}(\tau) &= \mathrm{Int}_2[G(x;x)G(x;x)],\\
P_{\rm e1}(\tau) &= \mathrm{Int}_2[G(x;x)G(x;x)],\\
P_{\rm f0}(\tau) &= \mathrm{Int}_2[G(y;y)G(y;y)],\\
P_{\rm f1}(\tau) &= \mathrm{Int}_2[G(y;y)G(y;y)],
\end{aligned} \tag{A33}$$

except for the coefficient in Eq. (A25), the coefficient in the brackets of Eq. (A8), the multiplicity of the spin component, and the statistical factor. Here the superscript in the partial differential symbol means

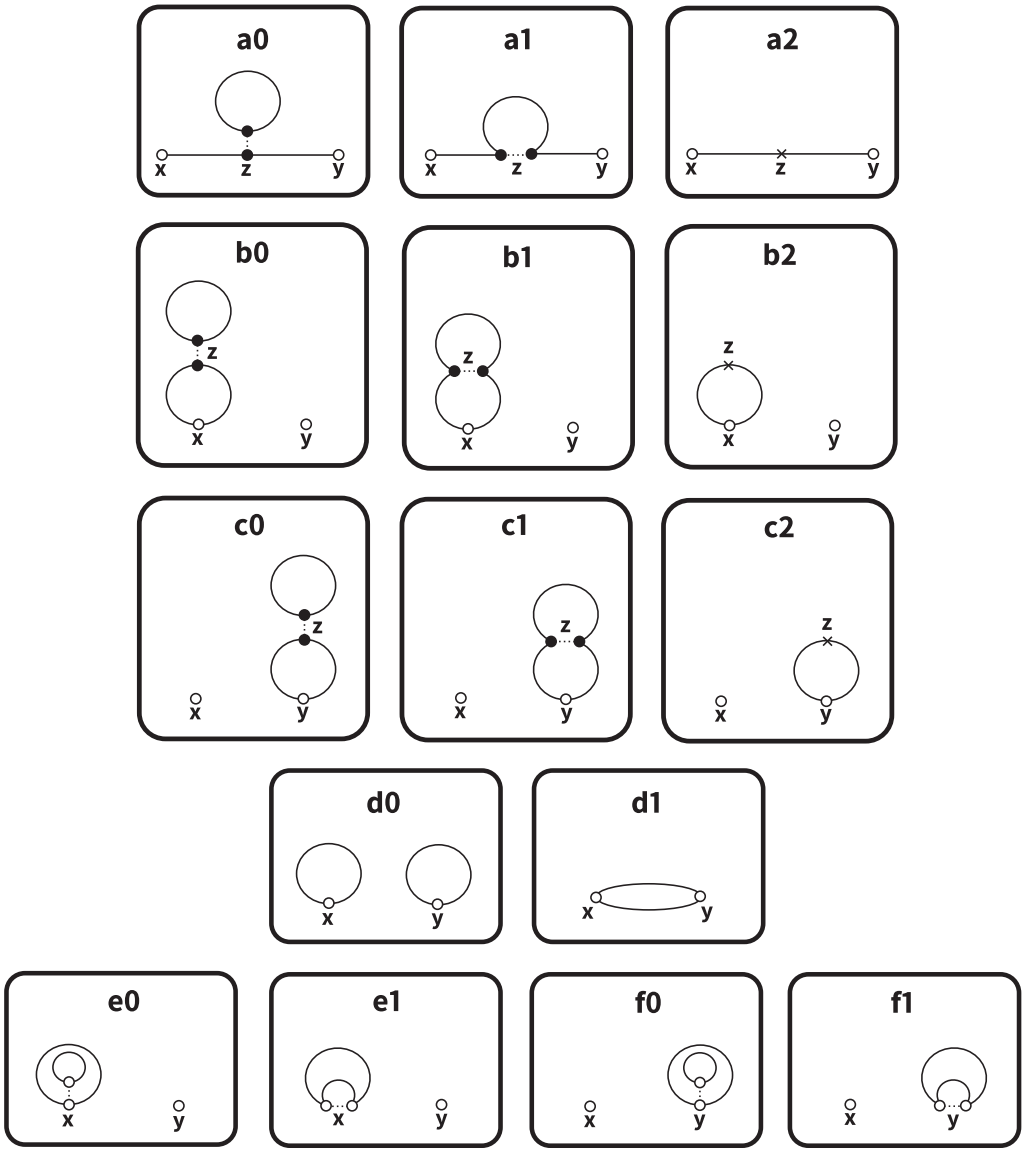

FIG. 9. The diagrammatic description of the $O(n)$-invariant two-point Green function at $\mathcal{O}(g^4)$.

$$\partial_\mu^1 G(u,v) \equiv \frac{\partial G(u,v)}{\partial u^\mu}, \quad \partial_\mu^2 G(u,v) \equiv \frac{\partial G(u,v)}{\partial v^\mu}. \tag{A34}$$

The explicit forms of each $P(\tau)$ in Eq. (A33) and the multiplying factor F are summarized in Table XIV. Note that $R(x_0 + y_0 \pm T, \boldsymbol{x} - \boldsymbol{y})$ in Eq. (A20) cannot be ignored for the derivation of some of the $P(\tau)$'s at this order. In addition, it should also be noted that $\partial_0^1 \partial_0^2 G_Z(x_0; y_0)|_{x_0=y_0} = \frac{1}{L^{d-1}}\delta(0)$ vanishes due to $\delta(0) = 0$ with the dimensional regularization.

The total contribution at $\mathcal{O}(g^4)$ can be written as

$$g^4 \frac{1}{L^{2(d-1)}} \int d^{d-1}\boldsymbol{x} \int d^{d-1}\boldsymbol{y} \langle \boldsymbol{\phi}(x) \cdot \boldsymbol{\phi}(y) \rangle_1 = g^4 \left[\frac{(n-1)}{2} R(0)^2 + (n-1) R(0) \left(\frac{|\tau|}{L^{d-1}} \right) + \frac{(n-1)^2}{2} \left(\frac{|\tau|}{L^{d-1}} \right)^2 \right]. \tag{A35}$$

TABLE XIV. The explicit forms of each $P(\tau)$ in Eq. (A33) and the multiplying factor F. The prime in $\sum_{\boldsymbol{p}}{}'$ means that the $\boldsymbol{p}=\boldsymbol{0}$ contribution is excluded from the summation. Note that $\frac{1}{2L^{d-1}}(\sum_{\boldsymbol{p}}{}'\frac{1}{\boldsymbol{p}^2})$ is nothing less than $R(0)$.

Diagram	$P(\tau)$	F
a0	$\frac{1}{L^{2(d-1)}}[(\frac{7\tau^4}{6T^2}-\frac{4\tau^3}{3T}+\frac{\tau^2}{12}+\frac{T^2}{1440})$	
	$+(\sum_{\boldsymbol{p}}{}'\frac{1}{\boldsymbol{p}^2})(-\frac{\tau^2}{2T^2}+\frac{1}{24})+(\sum_{\boldsymbol{p}}{}'\frac{1}{\boldsymbol{p}^4})(-\frac{3}{4T^2})]$	$-\frac{(n-1)^2g^4}{2}$
a1	$\frac{1}{L^{2(d-1)}}[(\frac{5\tau^4}{6T^2}-\frac{\tau^3}{T}+\frac{5\tau^2}{12}-\frac{T\tau}{12}+\frac{11T^2}{1440})$	
	$+(\sum_{\boldsymbol{p}}{}'\frac{1}{\lvert\boldsymbol{p}\rvert})(\frac{\tau^2}{2T}-\frac{\tau}{2}+\frac{T}{24})+(\sum_{\boldsymbol{p}}{}'\frac{1}{\boldsymbol{p}^4})(\frac{1}{4T^2})]$	$-(n-1)g^4$
a2	$\frac{1}{L^{d-1}}(-\frac{\tau^4}{3T}+\frac{2\tau^3}{3}-\frac{T\tau^2}{3}+\frac{T^3}{720})$	$-\frac{(n-1)^2g^4}{TL^{d-1}}$
b0	$\frac{1}{L^{2(d-1)}}[(\frac{7\tau^4}{6T^2}+\frac{\tau^2}{12}+\frac{T^2}{1440})+(\sum_{\boldsymbol{p}}{}'\frac{1}{\boldsymbol{p}^2})(-\frac{\tau^2}{2T^2}+\frac{1}{24})$	
	$+(\sum_{\boldsymbol{p}}{}'\frac{1}{\lvert\boldsymbol{p}\rvert^3})(-\frac{1}{2T})+(\sum_{\boldsymbol{p}}{}'\frac{1}{\boldsymbol{p}^4})(-\frac{3}{4T^2})]$	$+\frac{(n-1)^2g^4}{4}$
b1	$\frac{1}{L^{2(d-1)}}[(\frac{5\tau^4}{6T^2}-\frac{\tau^2}{12}+\frac{11T^2}{1440})+(\sum_{\boldsymbol{p}}{}'\frac{1}{\lvert\boldsymbol{p}\rvert})(\frac{\tau^2}{T}+\frac{T}{12})$	
	$+(\sum_{\boldsymbol{p}}{}'\frac{1}{\boldsymbol{p}^4})(\frac{1}{4T^2})+(\sum_{\boldsymbol{p}}{}'\frac{1}{\lvert\boldsymbol{p}\rvert})^2(\frac{1}{4})]$	$+\frac{(n-1)g^4}{2}$
b2	$\frac{1}{L^{d-1}}[(-\frac{\tau^4}{3T}+\frac{T\tau^2}{6}+\frac{T^3}{720})+(\sum_{\boldsymbol{p}}{}'\frac{1}{\lvert\boldsymbol{p}\rvert^3})(\frac{1}{4})]$	$+\frac{(n-1)^2g^4}{2TL^{d-1}}$
c0	$\frac{1}{L^{2(d-1)}}[(\frac{7\tau^4}{6T^2}+\frac{\tau^2}{12}+\frac{T^2}{1440})+(\sum_{\boldsymbol{p}}{}'\frac{1}{\boldsymbol{p}^2})(-\frac{\tau^2}{2T^2}+\frac{1}{24})$	
	$+(\sum_{\boldsymbol{p}}{}'\frac{1}{\lvert\boldsymbol{p}\rvert^3})(-\frac{1}{2T})+(\sum_{\boldsymbol{p}}{}'\frac{1}{\boldsymbol{p}^4})(-\frac{3}{4T^2})]$	$+\frac{(n-1)^2g^4}{4}$
c1	$\frac{1}{L^{2(d-1)}}[(\frac{5\tau^4}{6T^2}-\frac{\tau^2}{12}+\frac{11T^2}{1440})+(\sum_{\boldsymbol{p}}{}'\frac{1}{\lvert\boldsymbol{p}\rvert})(\frac{\tau^2}{T}+\frac{T}{12})$	
	$+(\sum_{\boldsymbol{p}}{}'\frac{1}{\boldsymbol{p}^4})(\frac{1}{4T^2})+(\sum_{\boldsymbol{p}}{}'\frac{1}{\lvert\boldsymbol{p}\rvert})^2(\frac{1}{4})]$	$+\frac{(n-1)g^4}{2}$
c2	$\frac{1}{L^{d-1}}[(-\frac{\tau^4}{3T}+\frac{T\tau^2}{6}+\frac{T^3}{720})+(\sum_{\boldsymbol{p}}{}'\frac{1}{\lvert\boldsymbol{p}\rvert^3})(\frac{1}{4})]$	$+\frac{(n-1)^2g^4}{2TL^{d-1}}$
d0	$\frac{1}{L^{2(d-1)}}[(\frac{\tau^2}{T}+\frac{T}{12})+(\sum_{\boldsymbol{p}}{}'\frac{1}{\lvert\boldsymbol{p}\rvert})(\frac{1}{2})]^2$	$+\frac{(n-1)^2g^4}{4}$
d1	$\frac{1}{L^{2(d-1)}}(\frac{\tau^2}{T}-\tau+\frac{T}{12})^2$	$+\frac{(n-1)g^4}{2}$
e0	$\frac{1}{L^{2(d-1)}}[(\frac{\tau^2}{T}+\frac{T}{12})+(\sum_{\boldsymbol{p}}{}'\frac{1}{\lvert\boldsymbol{p}\rvert})(\frac{1}{2})]^2$	$-\frac{(n-1)^2g^4}{8}$
e1	$\frac{1}{L^{2(d-1)}}[(\frac{\tau^2}{T}+\frac{T}{12})+(\sum_{\boldsymbol{p}}{}'\frac{1}{\lvert\boldsymbol{p}\rvert})(\frac{1}{2})]^2$	$-\frac{(n-1)g^4}{4}$
f0	$\frac{1}{L^{2(d-1)}}[(\frac{\tau^2}{T}+\frac{T}{12})+(\sum_{\boldsymbol{p}}{}'\frac{1}{\lvert\boldsymbol{p}\rvert})(\frac{1}{2})]^2$	$-\frac{(n-1)^2g^4}{8}$
f1	$\frac{1}{L^{2(d-1)}}[(\frac{\tau^2}{T}+\frac{T}{12})+(\sum_{\boldsymbol{p}}{}'\frac{1}{\lvert\boldsymbol{p}\rvert})(\frac{1}{2})]^2$	$-\frac{(n-1)g^4}{4}$

4. Evaluation of $R(\mathbf{0})$

Here we evaluate $R(0)$, which appears in Eqs. (A31) and (A35). The discussion in this subsection is based on Ref. [20]. From Eq. (A23), we have

$$\begin{aligned}R(z)&=\frac{1}{L^{d-1}}\sum_{\boldsymbol{q_n}\neq\boldsymbol{0}}\int_{-\infty}^{\infty}\frac{dq_0}{2\pi}\frac{1}{q_0^2+\boldsymbol{q_n}^2}e^{iq_0z_0+i\boldsymbol{q_n}\cdot\boldsymbol{z}}\\&=\int_0^{\infty}d\lambda\left[\int_{-\infty}^{\infty}\frac{dq_0}{2\pi}e^{-\lambda q_0^2+iq_0z_0}\right]\left[\frac{1}{L^{d-1}}\sum_{\boldsymbol{q_n}\neq\boldsymbol{0}}e^{-\lambda\boldsymbol{q_n}^2+i\boldsymbol{q_n}\cdot\boldsymbol{z}}\right]\\&=\int_0^{\infty}d\lambda[(4\pi\lambda)^{-\frac{1}{2}}e^{-\frac{z_0^2}{4\lambda}}]\left[(4\pi\lambda)^{-\frac{d-1}{2}}\sum_{\boldsymbol{w}\in\mathbb{Z}^{d-1}}e^{-\frac{(\boldsymbol{z}+L\boldsymbol{w})^2}{4\lambda}}-\frac{1}{L^{d-1}}\right].\end{aligned}\tag{A36}$$

We change the variable from λ to $u\equiv 4\pi\lambda/L^2$. Then, we have

$$R(z)\mu^{-(d-2)} = \frac{1}{4\pi(\mu L)^{d-2}}\int_0^\infty du u^{-\frac{1}{2}} e^{-\frac{\pi z_0^2}{L^2 u}} \times \left[u^{-\frac{d-1}{2}}\prod_{\mu=1}^{d-1}\left\{\sum_{w_\mu=-\infty}^{\infty} e^{-\pi\frac{(z_\mu/L+w_\mu)^2}{u}}\right\} - 1\right], \tag{A37}$$

where an arbitrary scale μ with dimensions of mass is introduced to make $R(z)$ dimensionless. μ is called the renormalization scale.

We consider the case where $z = 0$. We define the function

$$S(u) \equiv \sum_{n=-\infty}^{\infty} e^{-\pi u n^2}. \tag{A38}$$

Using the relation $S(u) = u^{-1/2}S(u^{-1})$, we obtain

$$R(0)\mu^{-(d-2)} = \frac{1}{4\pi(\mu L)^{d-2}}\int_0^\infty du u^{-1/2}[S(u)^{d-1} - 1]. \tag{A39}$$

Moreover, we introduce the notation

$$[f(u)]_{\rm sub} = \begin{cases} f(u) - [f(u)]_0 & (0 < u < 1), \\ f(u) - [f(u)]_\infty & (1 < u), \end{cases} \tag{A40}$$

where $[f(u)]_0$ and $[f(u)]_\infty$ denote the leading asymptotic parts of $f(u)$ at $u \to 0$ and $u \to \infty$, respectively. Then, Eq. (A39) can be rewritten as

$$R(0)\mu^{-(d-2)} = \frac{1}{2\pi(\mu L)^{d-2}}\left[-\frac{1}{d-2} - 1 + \frac{1}{2}\int_0^\infty du u^{-1/2}[S(u)^{d-1}]_{\rm sub}\right]. \tag{A41}$$

We expand $S(u)^{d-1}$ with respect to $(d-2)$, and obtain

$$R(0)\mu^{-(d-2)} = \frac{1}{2\pi(\mu L)^{d-2}}\left\{-\frac{1}{d-2} - 1 + \sum_{j=0}^{\infty}(d-2)^j\frac{X_j}{j!}\right\}, \tag{A42}$$

with

$$X_j \equiv \frac{1}{2}\int_0^\infty du u^{-1/2}[S(u)(\ln S(u))^j]_{\rm sub}. \tag{A43}$$

As we will see later, X_0 and X_1 do not appear in the final expression of the β function and anomalous dimension up to the $\mathcal{O}(g^6)$ order of the renormalization factor. Thus, we do not give the numerical values of X_0 and X_1. We add that X_0 can be written in an analytical form,

$$X_0 = 1 - \frac{1}{2}(\ln 4\pi + \Gamma'(1)). \tag{A44}$$

Finally, expanding $(\mu L)^{-(d-2)}$ with respect to $(d-2)$, we obtain

$$R(0)\mu^{-(d-2)} = \frac{1}{2\pi}\left\{-\frac{1}{d-2} + Y_0(\mu L) + (d-2)Y_1(\mu L) + \mathcal{O}((d-2)^2)\right\}, \tag{A45}$$

where we use the following functions:

$$Y_0(\mu L) \equiv (X_0 - 1) + (\ln \mu L), \tag{A46}$$

$$Y_1(\mu L) \equiv X_1 - (X_0 - 1)(\ln \mu L) - \frac{1}{2}(\ln \mu L)^2. \tag{A47}$$

5. Renormalization in the MS scheme

In Eq. (A25) [using Eqs. (A31) and (A35)], the $O(n)$-invariant two-point Green function was given as a series of the bare coupling g^2. It might be preferable to rewrite it in terms of the renormalized coupling. As the UV property is not affected by properties of the box such as the size or the boundary condition, it is possible to use the MS scheme for the renormalization. The $\mathcal{O}(g^6)$ renormalization factor of the $O(n)$ sigma model was already given in Ref. [25]. The renormalization is done by making the replacements

$$g^2\mu^{d-2} = Z^g_{\rm MS} g^2_{\rm MS}, \tag{A48}$$

$$\boldsymbol{\phi}(z) = (Z^\phi_{\rm MS})^{1/2}\boldsymbol{\phi}_{\rm MS}(z), \tag{A49}$$

with

$$Z^g_{\rm MS} = 1 + \frac{n-2}{2\pi(d-2)}g^2_{\rm MS} + \left[\frac{n-2}{8\pi^2(d-2)} + \frac{(n-2)^2}{4\pi^2(d-2)^2}\right]g^4_{\rm MS} + \left[\frac{(n-2)(n+2)}{96\pi^3(d-2)} + \frac{7(n-2)^2}{48\pi^3(d-2)^2} + \frac{(n-2)^3}{8\pi^3(d-2)^3}\right]g^6_{\rm MS} + \mathcal{O}(g^8_{\rm MS}), \tag{A50}$$

$$Z^\phi_{\rm MS} = 1 + \frac{n-1}{2\pi(d-2)}g^2_{\rm MS} + \frac{(n-1)(n-\frac{3}{2})}{4\pi^2(d-2)^2}g^4_{\rm MS} + \left[\frac{(n-1)(n-2)}{32\pi^3(d-2)} + \frac{(n-1)(n-2)}{24\pi^3(d-2)^2} + \frac{(n-1)(n^2-\frac{19}{6}n+\frac{5}{2})}{8\pi^3(d-2)^3}\right]g^6_{\rm MS} + \mathcal{O}(g^8_{\rm MS}). \tag{A51}$$

μ, which was introduced in Sec. A 4, is also used to make $g^2_{\rm MS}$ dimensionless. Note that the MS scheme focuses on only the

elimination of the UV divergence, and thus the coefficients in Eqs. (A50) and (A51) contain only the pole terms.

Using Eqs. (A48) and (A50), the zero-momentum projected $O(n)$-invariant Green function $G_{\rm inv}(x_0; y_0)|_{x_0=-\tau,y_0=+\tau}$ can be rewritten as

$$\begin{aligned}
&1+g_{\rm MS}^2\left[\left(\frac{n-1}{2\pi(d-2)}-\frac{n-1}{2\pi}Y_0(\mu L)-\frac{(d-2)(n-1)}{2\pi}Y_1(\mu L)\right)\right.\\
&\left.+(-(n-1)+(d-2)(n-1)(\ln\mu L))\left(\frac{|\tau|}{L}\right)\right]\\
&+g_{\rm MS}^4\left[\left(\frac{(n-1)(n-\frac{3}{2})}{4\pi^2(d-2)^2}-\frac{(n-1)^2}{4\pi^2(d-2)}Y_0(\mu L)\right.\right.\\
&\left.+\frac{n-1}{8\pi^2}Y_0(\mu L)^2-\frac{(n-1)^2}{4\pi^2}Y_1(\mu L)\right)\\
&+\left(-\frac{(n-1)^2}{2\pi(d-2)}+\frac{n-1}{2\pi}Y_0(\mu L)+\frac{(n-1)^2}{2\pi}(\ln\mu L)\right)\left(\frac{|\tau|}{L}\right)\\
&\left.+\frac{(n-1)^2}{2}\left(\frac{|\tau|}{L}\right)^2\right]+\mathcal{O}(g_{\rm MS}^6). \qquad \text{(A52)}
\end{aligned}$$

In Eq. (A52), we abbreviate $\mathcal{O}((d-2)^2)$ terms in the coefficient of $g_{\rm MS}^2$, and $\mathcal{O}(d-2)$ terms in that of $g_{\rm MS}^4$.

For the later discussion, we summarize the β function and the anomalous dimension. In general, the perturbative expression in the R scheme can be written as

$$\beta_{\rm R}(g_{\rm R}^2)=(d-2)g_{\rm R}^2-g_{\rm R}^4\sum_{i=0}^{\infty}g_{\rm R}^{2i}\beta_{{\rm R},i}, \qquad \text{(A53)}$$

$$\gamma_{\rm R}(g_{\rm R}^2)=-g_{\rm R}^2\sum_{i=0}^{\infty}g_{\rm R}^{2i}\gamma_{{\rm R},i} \qquad \text{(A54)}$$

with the dimensional regularization. For the MS scheme, each coefficient is given by

$$\beta_{{\rm MS},0}=\frac{n-2}{2\pi},\quad \beta_{{\rm MS},1}=\frac{n-2}{4\pi^2},\quad \beta_{{\rm MS},2}=\frac{(n-2)(n+2)}{32\pi^3}, \qquad \text{(A55)}$$

$$\gamma_{{\rm MS},0}=-\frac{n-1}{2\pi},\quad \gamma_{{\rm MS},1}=0,\quad \gamma_{{\rm MS},2}=-\frac{3(n-1)(n-2)}{32\pi^3}, \qquad \text{(A56)}$$

up to the $\mathcal{O}(g_{\rm MS}^6)$ order of the renormalization factor. $\beta_{{\rm MS},2}$ and $\gamma_{{\rm MS},2}$ were first derived in Ref. [25]. The derivation is straightforward from Eqs. (A48), (A50), and (A51).

6. Renormalization in the FV scheme

The zero-momentum projected $O(n)$-invariant Green function can be reexpressed using the mass gap M and the amplitude A as

$$G_{\rm inv}(x_0; y_0)|_{x_0=-\tau,y_0=+\tau}=Ae^{-2|\tau|M}. \qquad \text{(A57)}$$

Using the expansion

$$M=\sum_{i=1}^{\infty}g_{\rm MS}^{2i}M_i,\qquad A=1+\sum_{i=1}^{\infty}g_{\rm MS}^{2i}A_i, \qquad \text{(A58)}$$

the right-hand side of Eq. (A57) can be expanded as

$$\begin{aligned}
Ae^{-2|\tau|M}=1&+g_{\rm MS}^2\left[A_1-2LM_1\left(\frac{|\tau|}{L}\right)\right]\\
&+g_{\rm MS}^4\left[A_2-2L(A_1M_1+M_2)\left(\frac{|\tau|}{L}\right)\right.\\
&\left.+2L^2M_1^2\left(\frac{|\tau|}{L}\right)^2\right]+\mathcal{O}(g_{\rm MS}^6). \qquad \text{(A59)}
\end{aligned}$$

Comparing Eqs. (A52) and (A59), we obtain

$$\begin{aligned}
M_1&=\frac{n-1}{2L}-\frac{(d-2)(n-1)}{2L}(\ln\mu L),\\
M_2&=\frac{(n-1)(n-2)}{2L}\times\frac{1}{2\pi}Y_0(\mu L), \qquad \text{(A60)}
\end{aligned}$$

$$\begin{aligned}
A_1&=\frac{n-1}{2\pi(d-2)}-\frac{n-1}{2\pi}Y_0(\mu L)-\frac{(d-2)(n-1)}{2\pi}Y_1(\mu L),\\
A_2&=\frac{(n-1)(n-\frac{3}{2})}{4\pi^2(d-2)^2}-\frac{(n-1)^2}{4\pi^2(d-2)}Y_0(\mu L)\\
&\quad+\frac{n-1}{8\pi^2}Y_0(\mu L)^2-\frac{(n-1)^2}{4\pi^2}Y_1(\mu L). \qquad \text{(A61)}
\end{aligned}$$

We abbreviate $\mathcal{O}((d-2)^2)$ terms in M_1 and A_1, and $\mathcal{O}(d-2)$ terms in M_2 and A_2.

Until now, the perturbative evaluation of the mass gap in a finite box has been given at the $\mathcal{O}(g_{\rm MS}^4)$ order [13,16], the $\mathcal{O}(g_{\rm MS}^6)$ order [2,15,19], and the $\mathcal{O}(g_{\rm MS}^8)$ order [17]. The $\mathcal{O}(g_{\rm MS}^6)$ expression is

$$M=\frac{n-1}{2L}[g_{\rm MS}^2+g_{\rm MS}^4C_1+g_{\rm MS}^6C_2+\mathcal{O}(g_{\rm MS}^8)], \qquad \text{(A62)}$$

with

$$\begin{aligned}
C_1&=\frac{n-2}{2\pi}Y_0(\mu L),\\
C_2&=C_1^2+\frac{C_1}{2\pi}+\frac{3(n-2)}{16\pi^2}. \qquad \text{(A63)}
\end{aligned}$$

Our evaluation in Eq. (A60) is consistent with C_1 in Eq. (A63) at $d=2$.

The mass gap M does not depend on the arbitrarily introduced μ. This fact means that the μ dependence in C_i cancels with that in $g_{\rm MS}^2$, and M leaves only the L dependence. The situation is the same for the amplitude A.

We introduce the FV scheme. The μ and L dependences in each coefficient C_i appear only through the form of μL even at a higher order. Thus, if we set the renormalization scale by $\mu = 1/L$, the coefficient $c_i \equiv C_i|_{\mu=1/L}$ a constant independent of μ and L. Then, we can consider the new renormalized coupling

$$g^2_{\rm FV} = g^2_{\rm MS}\left(1 + \sum_{i=1}^{\infty} g^{2i}_{\rm MS} c_i\right). \tag{A64}$$

Moreover, with another constant coefficient $a_i \equiv A_i|_{\mu=1/L}$, we can introduce the new wave-function renormalization

$$Z^{\phi}_{\rm FV} = 1 + \sum_{i=1}^{\infty} g^{2i}_{\rm MS} a_i. \tag{A65}$$

These is nothing less than the renormalization in the FV scheme, which has been discussed in Sec. II B.

7. β function and anomalous dimension in the FV scheme

We discuss the β function and the anomalous dimension in the FV scheme. The β function in the FV scheme is converted from that in the MS scheme by

$$\beta_{\rm FV}(g^2_{\rm FV}) = \beta_{\rm MS}(g^2_{\rm MS})\frac{dg^2_{\rm FV}}{dg^2_{\rm MS}}. \tag{A66}$$

Substituting Eqs. (A53) and (A64) into Eq. (A66), at $d = 2$ we obtain

$$\begin{aligned} &\beta_{\rm FV,0} = \beta_{\rm MS,0}, \qquad \beta_{\rm FV,1} = \beta_{\rm MS,1}, \\ &\beta_{\rm FV,2} = \beta_{\rm MS,2} - \beta_{\rm MS,1} c_1 - \beta_{\rm MS,0}(c_2 - c_1^2), \end{aligned} \tag{A67}$$

up to $\mathcal{O}(g^6_{\rm MS})$ of the renormalization factor. Then, we have

$$\beta_{\rm FV,0} = \frac{n-2}{2\pi}, \quad \beta_{\rm FV,1} = \frac{n-2}{4\pi^2}, \quad \beta_{\rm FV,2} = \frac{(n-1)(n-2)}{8\pi^3} \tag{A68}$$

using Eqs. (A55) and (A63). We note that Eq. (A68) was first given in Ref. [2].

The anomalous dimension in the FV scheme is converted from that in the MS scheme by

$$\gamma_{\rm FV}(g^2_{\rm FV}) = \gamma_{\rm MS}(g^2_{\rm MS}) + \beta_{\rm MS}(g^2_{\rm MS})\frac{d}{dg^2_{\rm MS}}\ln\eta(g^2_{\rm MS}), \tag{A69}$$

with $\eta \equiv Z^{\phi}_{\rm FV}/Z^{\phi}_{\rm MS}$. The difference of the renormalization scheme only affects the finite part. Thus, in the expansion of

$$\eta = 1 + \sum_{i=1}^{\infty} g^{2i}_{\rm MS}\eta_i, \tag{A70}$$

each coefficient η_i has no pole terms at $d = 2$. In fact, the coefficients are

$$\eta_1 = -\frac{n-1}{2\pi}(X_0 - 1), \qquad \eta_2 = \frac{n-1}{8\pi^2}(X_0 - 1)^2 \tag{A71}$$

up to $\mathcal{O}(g^4_{\rm MS})$ from Eqs. (A51) and (A65). Substituting Eqs. (A53), (A54), (A64), and (A70) into Eq. (A69), we obtain

$$\begin{aligned} &\gamma_{\rm FV,0} = \gamma_{\rm MS,0}, \qquad \gamma_{\rm FV,1} = \gamma_{\rm MS,1} - \gamma_{\rm MS,0} c_1 + \beta_{\rm MS,0}\eta_1, \\ &\gamma_{\rm FV,2} = \gamma_{\rm MS,2} - 2\gamma_{\rm MS,1} c_1 - \gamma_{\rm MS,0}(c_2 - 2c_1^2) \\ &\qquad + \beta_{\rm MS,1}\eta_1 + \beta_{\rm MS,0}(2\eta_2 - \eta_1^2 - 2\eta_1 c_1) \end{aligned} \tag{A72}$$

up to $\mathcal{O}(g^6_{\rm MS})$ of the renormalization factor. Then, we have

$$\gamma_{\rm FV,0} = -\frac{n-1}{2\pi}, \qquad \gamma_{\rm FV,1} = 0, \qquad \gamma_{\rm FV,2} = 0, \tag{A73}$$

using Eqs. (A55), (A56), (A63), and (A71).

[1] M. Lüscher, Commun. Math. Phys. **105**, 153 (1986); Nucl. Phys. **B354**, 531 (1991).
[2] M. Lüscher, P. Weisz, and U. Wolff, Nucl. Phys. **B359**, 221 (1991).
[3] V. Efimov, Phys. Lett. B **33**, 563 (1970).
[4] M. Gell-Mann and M. Levy, Nuovo Cimento **16**, 705 (1960).
[5] A. M. Polyakov, Phys. Lett. B **59**, 79 (1975).
[6] A. A. Migdal, ZhETF **69**, 1457 (1975) [Sov. Phys. JETP **42**, 743 (1975)].
[7] E. Brézin and J. Zinn-Justin, Phys. Rev. Lett. **36**, 691 (1976); Phys. Rev. B **14**, 3110 (1976).
[8] E. Brézin, J. Zinn-Justin, and J. C. Le Guillou, Phys. Rev. D **14**, 2615 (1976).

[9] G. 't Hooft, Nucl. Phys. **B61**, 455 (1973).
[10] N. D. Mermin and H. Wagner, Phys. Rev. Lett. **17**, 1133 (1966).
[11] S. Elitzur, Nucl. Phys. **B212**, 501 (1983).
[12] F. David, Commun. Math. Phys. **81**, 149 (1981).
[13] M. Lüscher, Phys. Lett. B **118**, 391 (1982).
[14] P. Hasenfratz, Phys. Lett. B **141**, 385 (1984).
[15] E. G. Floratos and D. Petcher, Nucl. Phys. **B252**, 689 (1985).
[16] E. Brézin and J. Zinn-Justin, Nucl. Phys. **B257**, 867 (1985).
[17] D. S. Shin, Nucl. Phys. **B496**, 408 (1997).
[18] F. Niedermayer and C. Weiermann, Nucl. Phys. **B842**, 248 (2011).
[19] F. Niedermayer and P. Weisz, J. High Energy Phys. 04 (2016) 110.
[20] F. Niedermayer and P. Weisz, J. High Energy Phys. 06 (2016) 102.
[21] S. Capitani, M. Lüscher, R. Sommer, and H. Wittig, Nucl. Phys. **B544**, 669 (1999); **B582**, 762 (2000).
[22] S. C. Jimenez, M. Oka, and K. Sasaki (to be published).
[23] P. Hasenfratz and H. Leutwyler, Nucl. Phys. **B343**, 241 (1990).
[24] J. Zinn-Justin, *Quantum Field Theory and Critical Phenomena*, 4th ed. (Clarendon, Oxford, 2002).
[25] S. Hikami and E. Brézin, J. Phys. A **11**, 1141 (1978).